Published in final edited form as:
Bioorg Med Chem. 2011 November 15; 19(22): 6906–6918. doi:10.1016/j.bmc.2011.09.021.

Small molecule probes of the receptor binding site in the *Vibrio cholerae* CAI-1 quorum sensing circuit

Megan E. Bolitho[a,†,‡], **Lark J. Perez**[a,‡], **Matthew J. Koch**[a], **Wai-Leung Ng**[b], **Bonnie L Bassler**[b,c], and **Martin F. Semmelhack**[a,*]

Martin F. Semmelhack: mfshack@princeton.edu

[a]Department of Chemistry, Princeton University, Princeton, NJ 08544, USA

[b]Department of Molecular Biology, Princeton University, Princeton, NJ 08544, USA

[c]Howard Hughes Medical Institute, Chevy Chase, MD 20815, USA

Abstract

Based on modification of separate structural features of the *Vibrio cholerae* quorum sensing signal, (*S*)-3-hydroxytridecan-4-one (CAI-1), three focused compound libraries have been synthesized and evaluated for biological activity. Modifications to the acyl tail and α-hydroxy ketone typically provided agonists with activities correlated to tail length and conservative changes to the hydroxy ketone. Among the molecules identified within this collection of agonists is Am-CAI-1 (**B11**), which is among the most potent agonists reported to date with an EC_{50} of 0.21 μM. Modifications to the ethyl side chain delivered molecules with both agonist and antagonist activity, including *m*-OH-Ph-CAI-1 (**C13**) which is the most potent antagonist reported to date with an IC_{50} of 36 μM. The molecules described in this manuscript are anticipated to serve as valuable tools in the study of quorum sensing in *Vibrio cholerae* and provide new leads in the development of an antivirulence therapy against this human pathogen.

Keywords

Autoinducer; Quorum sensing; Structure-activity relationship; *Vibrio cholerae*; Agonist; Antagonist

1. Introduction

Bacteria, once viewed as independent, single-celled organisms, are now known to exhibit collective behaviors using a cell-to-cell communication process called quorum sensing (QS).[1] QS bacteria monitor population density through the production, release, and detection of extracellular signal molecules called autoinducers (AIs). As a population of QS bacteria grows, the concentration of AIs grows in proportion to cell number. When a threshold AI concentration is achieved, the bacteria detect the AI and initiate a signal transduction cascade that culminates in the population-wide induction and/or repression of target genes. This community-wide synchronization of gene expression results in changes in behaviors which are effective only when undertaken simultaneously by the group. QS-controlled traits include virulence factor production, bioluminescence, biofilm formation, and sporulation.

*Corresponding author. Tel: +1 609 9333789.
†Present address: University of San Francisco, 2130 Fulton Street, San Francisco, CA 94117-1080, USA.
‡These two authors contributed equally to this work.

The study of QS has implications for a more fundamental understanding of bacterial communities, the evolution of multicellular organisms, and the development of novel anti-virulence therapeutics against a variety of pathogens.[2]

The human pathogen *Vibrio cholerae* is responsible for the disease cholera, a severe diarrheal condition that is a source of public health concern in many regions of the underdeveloped world.[3] In *V. cholerae*, virulence factor production is controlled by QS.[4] *V. cholerae* possesss two parallel QS circuits, consisting of the receptors LuxPQ and CqsS, which respond to the autoinducers AI-2 ((2*S*,4*S*)-2-methyl-2,3,3,4-tetrahydroxytetrahydrofuran borate) and CAI-1 ((*S*)-3-hydroxytridecan-4-one), respectively.[5,6] The AI-2 quorum sensing circuit is present in diverse bacterial species and is used for inter-species communication.[7] The CAI quorum sensing circuit is restricted primarily to *Vibrio* species and is thus proposed to be used for inter-*Vibrio* communication.[8]

CAI-1 is produced by the acyl-CoA transferase CqsA (Fig. 1).[9] Extracellular CAI-1 is detected by the membrane-bound receptor, CqsS. At low cell density, and thus, low CAI-1 concentration, CqsS acts as a kinase that initiates a cascade, leading to phosphorylation and activation of the response regulator called LuxO. PhosphoLuxO activates expression of genes encoding four small regulatory RNAs (sRNAs, Qrr1–Qrr4). The Qrr sRNAs repress translation of the master QS transcription factor called HapR. Repression of HapR enables expression of genes encoding virulence factors and those required for biofilm formation, traits that are essential for *V. cholerae* to establish an infection in the host.[10] At high cell density, and thus high CAI-1 concentration, CAI-1 binds CqsS. This event converts CqsS to a phosphatase which reverses the flow of phosphate through the circuit, culminating in dephsophorylation and inactivation of LuxO. Production of the Qrr sRNAs ceases which allows the *hapR* mRNA to be translated. HapR represses genes required for virulence and biofilms and HapR activates expression of a protease that is required for *V. cholerae* to escape from the host back into the environment.[11] It is interesting to note that in contrast to many quorum sensing circuits where virulence factors are upregulated at high cell density, in *Vibrio cholerae* virulence factor production is attenuated at high cell density. Because CAI-1-mediated QS controls virulence in *V. cholerae*, manipulating CAI-1 production or detection is viewed as a possible route to a new anti-*V. cholerae* therapy.

In this manuscript, we use directed synthesis to explore systematically the structure/activity relationship (SAR) for CAI-1 and the CqsS receptor. For this purpose, we divide the structure of CAI-1 into three components: the ethyl side chain (C_1–C_2), the hydroxyketone functionality (C_3–C_4), and the acyl tail (C_4–C_{13}) (Fig. 2, top center). A preliminary understanding of the SAR between ligand and receptor emerged from our previous work on the structure of CAI-1 and the mechanism of its biosynthesis. Specifically, to establish the structure of active CAI-1, we prepared its enantiomer (*ent*-CAI-1, **A7**) and both enantiomers of the homologs with C_8- and C_9-acyl chains (Fig. 3, **A3–A6**).[6] We produced a second series that varied the heteroatom at C_3, replacing OH with =O, Cl, Br, SH, and NH_2 (Fig. 3, **B1, B8–B11**).[12] Modification of the C_1–C_2 unit revealed, for the first time, an antagonist of the CqsS receptor, the phenyl analog Ph-CAI-1, **C5**. With this small library of analogs, we recently examined the responses of *V. cholerae* CqsS mutants, as summarized in Figure 2.[13] In that study, we showed that modification of a specific amino acid residue in the CqsS ligand binding domain (C170F) has a strong effect on the activity of analogs differing in acyl tail length, while a distinct amino acid (F162) plays a critical role in recognizing the ethyl group (C_1–C_2). Substitution of F162 with a smaller amino acid (F162A) converts Ph-CAI-1 from an antagonist to an agonist. These preliminary studies uncovered some of the critical interactions between the small molecule ligand and the receptor CqsS, and provided us a starting point for the identification of new, more potent agonists and antagonists of this QS circuit. Here we expand on our initial series of CAI-1 analogs with a focus on the

activity of molecules toward the wild-type *V. cholerae* CqsS receptor. In the discussion below, the biological activities of the previously reported analogs are included to provide a comprehensive analysis of the SAR for CAI-1 and CqsS.

2. Results and discussion

2.1. Library design and synthesis

Using conventional solution phase procedures, we constructed focused libraries of CAI-1 analogs to probe the structural requirements for productive interaction with *V. cholerae* CqsS.

2.1.1. Library A: acyl tail analogs—Library A (Fig. 3A) was designed to test the response of the wild-type CqsS receptor to systematic changes in acyl tail chain length compared to the 10-carbon tail in the native ligand, CAI-1. The compounds in this library were synthesized in a four-step sequence from (*S*)-2-hydroxybutyrate (**2**) or its enantiomer (Scheme 1). Protection of the secondary alcohol and formation of Weinreb amide **3** allowed rapid incorporation of a variety of acyl tails through Grignard reagent addition; deprotection of the secondary hydroxyl group provided analogs **A1–A9**.

2.1.2. Library B: hydroxyketone analogs—The importance of the steric and electronic properties of the core α-hydroxyketone structural motif was probed with the eleven compounds of Library B (Fig. 3B). Because hydrogen bonding interactions are often key in ligand recognition and binding by receptor proteins, the position and identity of both the hydroxyl and the carbonyl of the (3,4)-α-hydroxyketone moiety of CAI-1 were predicted to be critical determinants in the interaction between CAI-1 and CqsS.

The CAI-1 diketone (**B1**) and diol (**B2,** 3:1 mixture of diastereoisomers; not separated) analogs were obtained from racemic CAI-1 via oxidation and reduction, respectively (Scheme 2). The isomeric α-hydroxyketone analog **B3** was synthesized by addition of the lithium anion of 2-ethyl-1,3-dithiane (5) to decanal followed by dithiane deprotection. The synthesis of the hydroxyl group analogs **B8–B11** proceeded through racemic tosylate **6**, as reported earlier.[12] As thiol **B10** readily oxidized in air leading to significant amounts of the corresponding disulfide, bioassay of this compound was performed under reducing conditions (25 μM dithiothreitol). The α-aminoketone **B11** was accessed through conversion of tosylate **6** to the corresponding azide followed by hydrogenation with concomitant protection of the free amine as the *tert*-butylcarbamate. These conditions were found to be critical; in the absence of *t*-Boc protection, significant dimerization (via imine formation) of the free amine (NH_2-CAI-1, **B11**) was observed during the hydrogenation step. Acidic deprotection followed by recrystallization from chloroform yielded the hydrochloride salt of **B11** as a white crystalline solid.

2.1.3. Library C: ethyl chain analogs—A 30-member library of analogs (Fig. 3C) was designed to explore the steric effects of the C_1–C_2 portion of CAI-1 on activity and to elaborate the SAR underlying the antagonism of phenylCAI-1 (**C5**) that we recently reported.[13] Analogs within this series were assembled as racemates by addition of the lithium anion of 2-nonyl-1,3-dithiane (**7**) to a series of appropriately functionalized aldehydes and subsequent deprotection of the dithiane (Scheme 3). Due to difficulties in performing this coupling reaction with acetaldehyde, compound **C1** was instead prepared from (*S*)-2-hydroxypropanoic acid in an manner analogous to that described for the assembly of Library A (see Section 4). Similarly, amino-phenyl derivative **C30** was prepared from the *t*-Boc-protected amino acid in an analogous sequence (see Section 4).

2.2. Primary bioassay data and SAR

2.2.1. Assay methods and analysis—To determine whether CAI-1 analogs can induce QS activity in *V. cholerae*, each molecule was added in triplicate to *V. cholerae* MM920 (Δ*cqsA*Δ*luxQ luxCDABE*) at increasing concentrations, and the light output from the reporter was monitored using a scintillation counter.[4] EC_{50} values were used to compare the relative activities (potency) of these agonists (Tables 1–3). The tables also present the % response for each analog. This latter parameter measures the maximum light output observed at saturation, and is compared to the maximum for CAI-1, set at 100%. Percent response does not necessarily correlate with potency as can be observed in Tables 1–3. Changes in the structure of the ligand or in the structure of the receptor binding site can alter the balance between kinase and phosphatase activities.[14]

Compounds that were ineffective as agonists were subsequently screened for antagonist activity by measuring the ability of the compound to reduce the response of the reporter to the native agonist, CAI-1. These experiments were performed by titrating increasing amounts of putative antagonists up to a concentration of 512 μM into wells containing the *V. cholerae* MM920 reporter in the presence of 1.0 μM CAI-1. Compounds that decreased the bioluminescence output were identified as antagonists. Cell growth was monitored by measuring OD_{600}; no growth inhibition was observed at the concentrations tested. IC_{50} values were used to compare the relative strengths (potency) of these antagonists (Table 4). The degree of decrease in light output at saturation differed among the active antagonists and these data are also provided in Table 4. The % inhibition is relative to CAI-1 which was set at 100%.

2.2.2. Library A: acyl tail analogs—The simple saturated acyl tail analogs report on the effect of alterations in the length of the acyl tail on signaling activity (Table 1). The pattern of agonist activities of this set of molecules demonstrates a distinct preference for the native 10-carbon acyl chain of CAI-1, in agreement with the trend suggested previously.[6] Both decreases (**A1–A6**) and increases (**A8–A9**) in the length of the acyl tail resulted in diminished agonist activity. The addition (e.g., **A8**) or removal (e.g., **A5**) of a single methylene group from the acyl chain results in a molecule capable of fully activating CqsS (100% response); however, these analogs require higher concentrations to achieve activity comparable to CAI-1 (EC_{50} values 8.4- and 4.6-fold higher, respectively). The removal of two methylene units from CAI-1, as in (*S*)-C8-CAI-1 (**A3**), results in a 39-fold decrease in activity along with a decrease in the maximal activation of CqsS to 83%. Consistent with this trend, both the addition and the removal of three methylene units result in striking reductions in activity, as molecules (*S*)-C7-CAI-1 (**A2**) and (*S*)-C13-CAI-1 (**A9**) are essentially inactive. These results suggest that although the CqsS receptor is somewhat promiscuous in its recognition of the saturated acyl tail in CAI-1 and analogs, there is a strict limit reached upon the addition or removal of three carbon units. The effect of changes in the acyl tail chain length on biological activity was examined by western blot against HapR and Tcp (see Supplementary data). As anticipated, CAI-1 (**1**) causes a significant reduction in the expression of Tcp with the concomitant expression of HapR and longer or shorter chain analogs of CAI-1 were reduced in the ability to induce this phenotype. In addition, the enantiomeric CAI-1 acyl tail analogs display approximately two-fold decreases in potency from their corresponding *S* counterparts (entries 3b, 4b, and 5b).

2.2.3. Library B: hydroxyketone analogs—Evaluation of Library B revealed a significant dependence of both EC_{50} and the percent maximal bioluminescence on variations in the α-hydroxyketone motif. Analogs **B1–B7** alternate the functionality at the C_3 and C_4 positions between=O, –OH, and –H. The diminished activities of these analogs support the hypothesis that this region of CAI-1, which bears the greatest structural complexity and

provides the opportunity for hydrogen bonding interactions with the receptor, tolerates only minor structural changes. Removal of functionality at either the 3- or **4**-position completely abolishes activity (**B4–B7**; Table 2, entries 5–8), but analogs that maintain an oxygen substituent at both positions retain modest agonist activity. Specifically, α-diketone **B1** (entry 2) and α-diol **B2** (entry 3) both show activation comparable to CAI-1, but only at high concentration; they are significantly less potent, with EC_{50} values at least an order of magnitude greater than that of CAI-1. The isomeric α-hydroxyketone **B3** (entry 4) is significantly weaker in terms of both receptor activation (38% response) and potency (EC_{50} 84-fold higher). The less active isomer may be relevant in the duration of the QS response in *V. cholerae*. In our synthesis efforts, isomerization of CAI-1 to **B3** was noted during a variety of reaction conditions. While the rate of this process is not high during in vitro storage, there is evidence that the isomerization may be facilitated in vivo; it may serve as a mechanism of inactivation of the signal.[12] Compounds **B8–B11**, in which the 3-position hydroxyl of CAI-1 was modified, show varied permissibility for substitution of the –OH group with other heteroatoms (entries 9–12). For example, while chloride **B8** is inactive, bromide **B9** and thiol **B10** are both active, albeit with potency decreases of roughly 10-fold from CAI-1. Both **B9** and **B10** exhibit a substantial loss of maximum response (73% and 67%, respectively). By contrast, the α-amino ketone **B11** displays activity equal to CAI-1, with an EC_{50} value of 210 nM and achieving 105% response. This result was initially surprising, but subsequent analyses of the CAI-1 biosynthetic mechanism indicate that introduction of an amino group at C_3 may be a step in the in vivo biosynthesis of the autoinducer.[12] This pathway and the significance of NH_2-CAI-1 in *V. cholerae* QS are currently under investigation.[9]

2.2.4. Library C: ethyl chain analogs—Library C analogs all contain modifications to the C_1–C_2 region of CAI-1. Both agonist and antagonist activities were observed among these molecules. Saturated hydrocarbon analogs within this library typically acted as agonists (Table 3). In contrast, substitution of the ethyl side chain of CAI-1 with phenyl moieties resulted in antagonists of CqsS (Table 4).

2.2.4.1. Ethylchain analog agonists: Among the saturated hydrocarbon ethyl chain analogs **C1–C4**, the Me-CAI-1 analog (**C1**) possessing a side chain one carbon shorter than CAI-1 showed nearly the same agonist activity as the native autoinducer, both in potency (EC_{50} 2.6-fold higher) and level of maximum bioluminescence (Table 3, entry 1). The analog with an *n*-propyl side chain (**C2,** entry 3) was a moderately effective agonist, achieving 84% of the native maximal bioluminescence of CAI-1 with an EC_{50} value 6-fold higher. These observations are consistent with those made in Library A, in which the conservative removal or addition of a single methylene unit is generally tolerated while more dramatic alterations in the CAI-1 backbone structure are not tolerated. Here, substituent branching is shown to dramatically decrease activity; *i*-Pr-CAI-1 (**C3**) is a poor agonist (21-fold decrease in potency) and *t*-Bu-CAI-1 (**C4**) is inactive.

2.2.4.2. Ethyl chain analog antagonists: The only activity exhibited by any of the aliphatic ethyl end analogs (**C1–C4**) is agonism. Upon substitution with an aromatic moiety, as in analogs **C5–C29**, the activity is switched to antagonism. The Ph-CAI-1 antagonist **C5** was recently reported to be a competitive inhibitor of CqsS.[13] In Table 4, we compare the activities of Ph-CAI-1 analogs to investigate the steric and electronic features that influence the antagonism activity of this class of molecules toward CqsS.

A variety of substituted phenyl analogs were evaluated which differ in steric and electronic effects of the substituents. From the behaviors of analogs **C6–C28,** it is apparent that the level of response and the potency of these molecules as antagonists are sensitive to the

nature of the substituents, but a general correlation is less clear. Increasing steric demands have a detrimental effect on antagonism (compare **C8–C11**). While the *p*-Me-Ph-CAI-1 (**C8**) analog is a moderate antagonist providing complete inhibition of CqsS with an IC_{50} value of 114 μM, the more sterically demanding analogs *p*-Et-Ph-CAI-1 (**C10**) and *p*-Pr-Ph-CAI-1 (**C11**) are inactive. Imposing the comparatively small steric demand of a methyl group at an additional position to give 3,4-di-Me-Ph-CAI-1 analog **C9** abolishes activity (compare Table 4, entries 4 and 5).

The potency of the methyl-substituted aryl analogs (**C6–C8**) as antagonists is highly dependent upon the position of the arene substitution. Here, the *meta*-substituted analog is most potent, followed in turn by the *para*-substituted and the *ortho*-substituted analog. This trend suggests the presence of a binding pocket in CqsS that can best accommodate the *meta*-substituted arene. This trend is also clear for the *ortho*-, *meta*-, *para*-OH-Ph-CAI-1 analog series (**C12–C14**). These electron-rich analogs exhibit among the highest activities of the analogs tested. All three molecules are capable of full inhibition (>100%) with high potency. In fact, *m*-OH-Ph-CAI-1 **C13** is a more potent inhibitor than the original Ph-CAI-1 antagonist **C5** (IC_{50} of 36 μM). The *p*-OH analog **C14** is less potent but still a good antagonist at IC_{50} = 78 μM, and the *o*-OH analog **C12** is the least potent at IC_{50} = 172 μM. Similar to the pattern obtained with methyl substitution, the addition of a second –OH substituent results in decreased antagonism, although 3,4-di-OH-Ph-CAI-1 **C15** is still a moderately potent antagonist (IC_{50} = 174 μM). The –OH group provides strong electron donation and an opportunity for hydrogen bonding.

Electron donation alone appears not to be a primary factor in strength of antagonism, as analogs bearing an –OMe group (**C16–C18**) are universally inactive (entries 12–14), although we note that the increased steric demands of these substituents may also be a factor in their lack of activity. The steric effect would be predicted to be similar to an ethyl group as in the analog *p*-Et-Ph-CAI-1, **C10** which is likewise inactive.

Three series of halogenated arenes were constructed using fluoro-, chloro-, and bromo-substituents to investigate the effect on antagonism of electron-withdrawal from the arene ring. The chlorine- and bromine-substituted arene molecules (**C23–C28**) are generally inactive with the exception of *p*-Br-Ph-CAI-1 (**C28**), which is a weak antagonist. Interestingly, the activity of the *para*-substituted analog is not in keeping with the trend implicating a *meta*-preference as exhibited by the tolyl (PhMe) and phenol (PhOH) series. The inactivity of the chloro- and bromo-substituted phenyl-CAI-1 analogs contrasts with that of the fluoro-substituted phenyl-CAI-1 analogs **C19–C21**, which are all active. Although less potent than original antagonist **C5** and phenol derivatives **C12– C14**, the *o*-, *m*-, and *p*-F-Ph-CAI-1 (**C19–C21**) analogs all exhibit high potency and are capable of fully inhibiting CqsS. The *ortho*-fluoro analog is the most potent in this case, followed by the *para*-and then the *meta*-substituted analogs. Also in contrast to the trend noted in the tolyl and phenol series, the substitution effects in the fluoro series appear to be relatively additive; the 2,5-di-F-Ph-CAI-1 analog (**C22**) shows enhanced potency compared to the mono-fluoro analogs. However, this antagonist is only capable of 48% inhibition compared to Ph-CAI-1. Taken together, these results suggest a difference in binding modes for the two series of analogs with the Me-Ph-CAI-1 and the HO-Ph-CAI-1 analogs forming one class and the F-Ph-CAI-1 analogs forming a second class.

The positioning of the phenyl ring on C_2 of CAI-1 (Ph-CAI-1 **C5**, entry 1) results in a more potent antagonist (IC_{50} of 55 μM for complete inhibition) than the attachment of the phenyl ring to C_1 of CAI-1 (**C29**, entry 25, IC_{50} of 136 μM for complete inhibition). Interestingly, while the conversion of the 3-OH group in CAI-1 to an $–NH_2$ group gave an analog (**B11**)

comparable in potency and response level as an agonist (Table 2, entry 12), the same functional group exchange in Ph-CAI-1 eliminated all inhibitory activity (Table 4, entry 26).

3. Conclusion

Three libraries of rationally designed analogs of the CAI-1 autoinducer of *V. cholerae* were prepared to probe the structure/activity relationship between the ligand and the CqsS receptor. Agonists typically consisted of a saturated, linear hydrocarbon backbone bearing a core α-hydroxyketone. While the presence of this core structural motif is significant for potency and activation of CqsS, some conservative changes are tolerated. Most notably, an α-amino ketone serves as an effective mimic of CAI-1 with approximately the same potency. Small changes in the overall chain length of the hydrocarbon backbone of CAI-1 are also tolerated; molecules with a total linear backbone length of 11–14 carbons are generally agonists. However, extending the CAI-1 backbone chain to a total of 16 carbons results in loss of activity, as does a shortening to fewer than 11 carbons or the introduction of branched structures at the ethyl end. In no case, however, did the addition or removal of saturated carbon units to the CAI-1 backbone or functional group changes at C_3 result in a molecule that behaved as an antagonist.

Drawing from our initial observations of the inhibitory activity of Ph-CAI-1 (**C5**),[13] we evaluated a series of aryl-CAI-1 analogs in which one or two substituents were positioned on the aryl ring. Among the most potent antagonists are *m*-Me-Ph-CAI-1 (**C7**), *m*-HO-Ph-CAI-1 (**C13**), and (2,5-di-F-Ph)-CAI-1 (**C22**). The *m*-hydroxyphenyl-CAI-1 analog (**C13**) is the most potent CqsS antagonist identified to date. The antagonist activity is sensitive to the steric and electronic features of the analog, but further structural information on the receptor will be required to generate a predictive model.

All of the antagonists discovered here contain a phenyl substituent. It is unclear at this time what the nature of the interaction is that leads to antagonism in these species. We recently reported chemical genetics studies with CqsS which led to the proposal that the arene portion of the Ph-CAI-1 ligand makes direct contact with a pair of phenylalanine residues in the sixth CqsS transmembrane helix, and it is possible that some manner of π-stacking interaction could be operative in mediating antagonism.[13] It is known that π-stacking interactions are highly dependent on the electronics of the systems involved and thus, changes in the electronics of the substituents on the arene on the ligand could alter these stacking interactions.[15] The precise contacts that are required to promote an antagonized or agonized receptor phenotype are currently under investigation and will hopefully define the preferred binding mode of the antagonists described within this series as well as their mechanism of antagonism.

The initiative reported here, which produced analogs of CAI-1 displaying both potent agonist and antagonist activities, has produced a deep understanding of the *V. cholerae* QS circuit. For example, the unexpectedly high potency of amino-CAI-1 (**B11**) inspired the idea that an amine-containing CAI-1-like compound may be a natural step in the CAI-1 biosynthetic mechanism.[9,12] Antagonist Ph-CAI-1 (**C5**) was used to identify ‘gatekeeper’ amino acid residues in the CqsS transmembrane domain that enabled insight into to the requirement for signal fidelity and the mechanism of CqsS signal transduction.[13] Acyl-tail analogs were used in an investigation of polymorphisms in CqsS receptors across *Vibrio* species to determine ligand preferences.[8] It is expected that the new agonists and antagonists described here will find utility in studies of *V. cholera* QS, and serve as new probes to investigate virulence and signaling.

4. Experimental

4.1. Vibrio cholerae agonism bioassay

Reporter strain MM920 (*V. cholerae* Δ*cqsA* Δ*luxQ* carrying pBB1 cosmid, which contains the *V. harveyi luxCDABE* luciferase operon) was used to assay agonist activity of each synthetic compound. This strain was grown in LB medium containing 10 μg/mL tetracycline at 30 °C for >16 h and diluted 20-fold with the same medium. Two microlitre of each synthetic compound dissolved in DMSO in various concentrations (maximum concentration tested = 51.2 μM) was added to 200 μL of the diluted reporter strain in triplicate in a 96-well plate. Bioluminescence and OD_{600} were measured in a PerkinElmer EnVision Multilabel Reader following 4-h incubation at 30 °C with shaking. DMSO was used as the negative control.

4.2. *Vibrio cholerae* antagonism bioassay

Reporter strain MM920 was used to assay the antagonist activity of each synthetic compound. This strain was grown in LB medium containing 10 μg/mL tetracycline at 30 °C for >16 h and diluted 20-fold with the same medium. CAI-1 is added to the diluted reporter at the final concentration of 1 μM. Two microlitre of each synthetic compound dissolved in DMSO in various concentrations (maximum concentration tested = 512 μM) was added to 200 μL of the diluted reporter strain in triplicate in a 96-well plate. Bioluminescence and OD_{600} were measured in a PerkinElmer EnVision Multilabel Reader following 4-h incubation at 30 °C with shaking. DMSO was used as the negative control.

4.3. Analytical methods

NMR spectra were recorded using a Varian Unity/Mercury 300 spectrometer (300 MHz for ^{1}H), a Varian Unity/Inova 400 spectrometer (400 MHz for ^{1}H), a Varian Unity/INOVA 500 spectrometer (500 MHz for ^{1}H; 125 MHz for ^{13}C), or a Bruker Avance II (500 MHz for ^{1}H; 125 MHz for ^{13}C) spectrometer fitted with either a ^{1}H-optimized TCI (H/C/N) cryoprobe or a ^{13}C-optimized dual C/H cryoprobe. Chemical shifts are reported in parts per million (ppm) and were calibrated according to residual protonated solvent. High-resolution mass spectral analysis was performed using an Agilent 1200-series electrospray ionization-time-of-flight (ESI-TOF) mass spectrometer in the positive ESI mode or was performed by Dr. John Eng (Princeton University) using a Kratos MS50 EI-HRMS. Low-resolution mass spectral analysis was performed by either Dr. Dorothy Little or Dr. John Eng (Princeton University) using a Kratos MS50 mass spectrometer in electron impact (EI) mode.

4.4. Chemical reactions

Unless otherwise noted, all reactions were performed in flame-dried glassware under an atmosphere of nitrogen or argon using dried reagents and solvents. All chemicals were purchased from commercial vendors and used without further purification. Diethyl ether (Et_2O) and tetrahydrofuran (THF) were dried by distillation from sodium benzophenone ketyl under argon. Dichloromethane (DCM) was distilled from calcium hydride (CaH_2) under argon. Other anhydrous solvents were purchased from commercial vendors.

4.5. Purification

Flash chromatography was performed using standard grade Silica Gel 60 230–400 mesh from SORBENT Technologies. Silica gel was loaded into glass columns as a slurry. Analytical thin-layer chromatography was carried out using Silica G TLC plates, 200 μm with UV_{254} fluorescent indicator (SORBENT Technologies), and visualization was performed by staining and/or by absorbance of UV light. Preparative thin-layer chromatography was carried out using SIL G-200 pre-coated glass TLC plates, 2.0 mm with

UV_{254} fluorescent indicator (Macherey-Nagel). High-performance liquid chromatography was performed using a Rainin HPLC with SD-1 pumps and a Dynamax UV-1 detector. Supercritical fluid chromatography was performed by Christina Kraml (Lotus Separations, LLC) using a Berger Multigram II SFC with Rainin SD-1 pumps and a Knauer K-2501 spectrophotometer.

4.6. Chemical synthesis

4.6.1. Library A synthesis—For the synthesis of compounds **A3–A7** and CAI-1, see Ref. 6.

4.6.1.1. (*S*)-2-(*tert*-Butyldimethylsilyloxy)-*N*-methoxy-*N*-meth-ylbutanamide: To a solution of (*S*)-2-hydroxybutyric acid (387 mg, 3.71 mmol) in DMF (2.5 mL) at room temperature was added imidazole (760 mg, 11.2 mmol) and TBSCl (1.68 g, 11.2 mmol), sequentially. The mixture was allowed to stir at room temperature for 18 h, then was diluted with Et_2O (20 mL) and quenched with 6 N HCl (10 mL). The resulting biphasic mixture was stirred vigorously for 15 min, the layers were separated and the aqueous layer was extracted with Et_2O (3 × 20 mL). The combined organic fractions were washed with water (2 × 20 mL) and brine (20 mL), dried over Na_2SO_4 and concentrated. The residue was treated with $SOCl_2$ (1.62 mL, 22.3 mmol) at room temperature and allowed to stir for 4 h before concentration in vacuo. The residue was dissolved in CH_2Cl_2 (10 mL) and was treated with *N,O*-dimethylhydroxylamine hydrochloride (724 mg, 7.42 mmol) and Et_3N (2.1 mL, 14.8 mmol) and allowed to stir for 14 h at rt. The reaction was concentrated to remove volatiles and was purified by silica gel chromatography eluting with hexanes to 40% EtOAc/hexanes to provide (*S*)-2-(*tert*-butyldimethylsilyloxy)-*N*-methoxy-*N*-methylbutanamide (445 mg, 46% over three steps). ^{1}H NMR (500 MHz, CDCl3) δ 4.42 (app s, 1H), 3.67 (s, 3H), 3.18 (s, 3H), 1.75-1.58 (m, 2H), 0.94 (t, J=7.4Hz, 3H), 0.88 (s, 9H), 0.06 (s, 3H), 0.04 (s, 3H).^{13}C NMR (125 MHz, $CDCl_3$) δ 169.9, 77.1, 61.5, 27.9, 26.0, 18.6, 10.4, −4.5, −4.9. HRMS (ESI-TOF) calcd for $C_{12}H_{28}NO_3Si$, 262.1839; observed 262.1847 $[M+H]^+$.

4.6.1.2. Compounds TBS-A1, TBS-A2, TBS-A8, and TBS-A9; general procedure: To a solution of (*S*)-2-(*tert*-butyldimethylsilyloxy)-*N*-methoxy-*N*-methylbutanamide (0.1 M in THF) at 0 °C was added the appropriate alkylmagnesium bromide (4 equiv). The reaction mixture was allowed to stir at 0 °C until the starting material had been consumed by TLC analysis (4–7 h). The mixture was diluted with diethyl ether and quenched with sat. NH_4Cl. The organic layer was separated and washed with 10% $KHSO_4$ and brine. The organic layer was then dried over Na_2SO_4, filtered, concentrated, and purified by silica gel column chromatography (hexanes to 10% EtOAc/hexanes) to give the desired product. Yields for this reaction were typically between 58% and 76%.

4.6.1.2.1. (S)-3-(tert-Butyldimethylsilyloxy)nonan-4-one, TBS-A1: ^{1}H NMR (500 MHz, C_6D_6) δ 3.92 (dd, J=6.8, 5.2 Hz, 1H); 2.52–2.36 (m, 2H); 1.68–1.58 (m, 3H); 1.55–1.46 (m, 1H); 1.29–1.16 (m, 4H); 0.96 (s, 9H); 0.87–0.83 (m, 6H); 0.00 (s, 3H); −0.03 (s, 3H). ^{13}C NMR (125 MHz, C_6D_6) δ 212.2, 80.5, 37.9, 32.2, 28.4, 26.3, 23.6, 23.3, 18.7, 14.5, 9.9, −4.5, −4.6. HRMS (ESI-TOF) calcd for $C_{15}H_{33}O_2Si$, 273.2250; observed 273.2256 $[M+H]^+$.

4.6.1.2.2. (S)-3-(tert-Butyldimethylsilyloxy)decan-4-one, TBS-A2: ^{1}H NMR (500 MHz, C_6D_6) δ 3.93 (dd, J=6.8, 5.2 Hz, 1H); 2.55–2.37 (m, 2H); 1.70–1.59 (m, 3H); 1.56–1.48 (m, 1H); 1.31–1.18 (m, 6H); 0.96 (s, 9H); 0.89–0.83 (m, 6H); 0.01 (s, 3H); −0.03 (s, 3H). ^{13}C NMR (125 MHz, C_6D_6) δ 212.2, 80.5, 37.9, 32.4, 29.8, 28.5, 26.3, 23.9, 23.3, 18.7, 14.6, 9.9, −4.5, −4.6. HRMS (ESI-TOF) calcd $C_{16}H_{35}O_2Si$, 287.2406; observed 287.2402 $[M+H]^+$.

4.6.1.2.3. (S)-3-(tert-Butyldimethylsilyloxy)tetradecan-4-one, TBS-A8: ^{1}H NMR (500 MHz, C_6D_6) δ 3.94(dd J = 6.7, 5.2 Hz, 1H); 2.57–2.41 (m, 2H); 1.73–1.60 (m, 3H); 1.57–1.47 (m, 1H); 1.34–1.21 (m, 14H); 0.96 (s, 9H); 0.92 (t, J = 7.0 Hz, 3H); 0.87 (t, J = 7.4 Hz, 3H); 0.01 (s, 3H), −0.03 (s, 3H). ^{13}C NMR (125 MHz, C_6D_6) δ 212.2, 80.5, 37.9, 32.7, 30.4, 30.3, 30.3, 30.2, 30.1, 28.5, 26.3, 24.0, 23.5, 18.7, 14.8, 9.9, −4.5, −4.6. HRMS (ESI-TOF) calcd for $C_{20}H_{43}O_2Si$, 343.3032; observed 343.3036 $[M+H]^+$.

4.6.1.2.4. (S)-3-(tert-Butyldimethylsilyloxy)hexadecan-4-one, TBS-A9: ^{1}H NMR (500 MHz, C_6D_6) δ 3.94(dd, J = 6.7, 5.2 Hz, 1H); 2.57–2.40 (m, 2H); 1.75–1.60 (m, 3H); 1.57–1.48 (m, 1H); 1.35–1.24 (m, 18H); 0.97 (s, 9H); 0.92 (t, J = 6.9 Hz, 3H); 0.87 (t, J = 7.4 Hz, 3H); 0.02 (s, 3H); −0.03 (s, 3H). ^{13}C NMR (125 MHz, C_6D_6) δ 212.2, 80.5, 37.9, 32.7, 30.5, 30.4, 30.4, 30.3, 30.2, 30.1, 28.5, 26.3, 24.0, 23.5, 18.7, 14.8, 9.9, −4.5, −4.6. HRMS (ESI-TOF) calcd for C22$H_{47}O_2Si$, 371.3345; observed 371.3346 $[M+H]^+$.

4.6.1.3. CompoundsA1, A2, A8, and A9; general procedure: To a solution of TBS-protected α-hydroxyketone (0.5 M in THF) at 0 °C was added tetrabutylammonium fluoride (1 M in THF, 3 equiv). The reaction mixture was warmed to room temperature, and progress of the reaction was monitored by TLC (4–18 h). The reaction was quenched by the addition of silica gel to make a thick slurry. This slurry was directly purified by silica gel chromatography using a gradient from hexanes to 20% EtOAc/hexanes to provide the desired product. Yields for this reaction were typically between 76% and 82%.

4.6.1.3.1. (S)-3-Hydroxynonan-4-one (A1): ^{1}H NMR (500 MHz, $CDCl_3$) δ 4.14 (dt, J = 6.7, 4.4 Hz, 1H); 3.49 (d, J = 4.7Hz, 1H); 2.49– 2.37 (m, 2H); 1.93–1.84 (m, 1H); 1.65–1.53 (m, 3H); 1.34–1.20 (m, 4H); 0.91 (t, J =7.4 Hz, 3H); 0.87 (t, J =7.0 Hz, 3H). ^{13}C NMR (125 MHz, $CDCl_3$) δ 212.7, 77.3, 38.0, 31.6, 26.9, 23.5, 22.6, 14.1, 9.0. HRMS (ESI-TOF) calcd for $C_9H_{19}O_2$, 159.1385; observed 159.1381 $[M+H]^+$.

4.6.1.3.2. (S)-3-Hydroxydecan-4-one (A2): ^{1}H NMR (500 MHz, $CDCl_3$) δ 4.14 (app s, 1H); 3.49 (s, 1H); 2.48–2.37 (m, 2H); 1.94–1.84 (m, 1H); 1.64–1.54 (m, 3H); 1.33–1.20 (m, 6H); 0.92 (t, J = 7.4 Hz, 3H); 0.86 (t, J = 6.4 Hz, 3H). ^{13}C NMR (125 MHz, $CDCl_3$) δ 212.7, 77.3, 38.1, 31.7, 29.1, 26.9, 23.8, 22.7, 14.3, 9.1. HRMS (ESI-TOF) calcd for $C_{10}H_21O_2$, 173.1542; observed 173.1545 $[M+H]^+$.

4.6.1.3.3. (S)-3-Hydroxytetradecan-4-one (A5): ^{1}H NMR(500 MHz, $CDCl_3$) δ 5.28 (s, 1H); 4.14 (dd, J = *6.7,* 4.0 Hz, 1H);2.48–2.37 (m, 2H); 1.93–1.84 (m, 1H); 1.64–1.54 (m, 3H); 1.32–1.19 (m, 14H); 0.91 (t, J =7.4 Hz, 3H); 0.85 (t, J = 6.9 Hz, 3H). ^{13}CNMR (125 MHz, $CDCl_3$) δ 212.7, 77.3, 38.0, 32.1, 29.8, 29.7, 29.6, 29.5, 29.4, 26.9, 23.8, 22.9, 14.4, 9.1. HRMS (ESI-TOF) calcd for $C_{14}H_{29}O_2$, 229.2168; observed 229.2172 $[M+H]^+$.

4.6.1.3.4. (S)-3-Hydroxyhexadecan-4-one (A6): ^{1}H NMR(500 MHz, $CDCl_3$) δ 5.28 (s, 1H); 4.14 (dd, J = 6.7, 4.0 Hz, 1H);2.49–2.37 (m, 2H); 1.92–1.83 (m, 1H); 1.62–1.54 (m, 3H); 1.32–1.16 (m, 18H); 0.91 (t, J =7.4 Hz, 3H); 0.85 (t, J = 6.9 Hz, 3H). ^{13}CNMR (125 MHz, $CDCl_3$) δ 212.7, 77.3, 38.1, 32.1, 29.8, 29.8, 29.8, 29.6, 29.6, 29.4, 26.9, 23.8, 22.9, 14.4, 9.1. HRMS (ESI-TOF) calcd for $C_{16}H_{33}O_2$, 257.2481; observed 257.2480 $[M+H]^+$.

4.6.2. Library B synthesis—For the synthesis of compounds **B1** and **B8–B11**, see Ref. 12. For an improved synthesis of compound **B11** see Ref. 13.

4.6.2.1. 3,4-Tridecanediol (B2): Sodium borohydride (0.923 g, 24.4 mmol) was added to a solution of racemic 3-hydroxytridec-an-4-one, (1.0 g, 4.8 mmol) in MeOH (19 mL) at 0 °C The mixture was warmed to 23 °C and monitored by TLC (20% EtOAc in hexanes). Upon

completion, the reaction mixture was acidified to pH 3 with 1 M sulfuric acid at 0 °C. The acidified solution was then diluted with 100 mL DCM, dried over magnesium sulfate, filtered, concentrated, and purified by silica gel chromatography (25% EtOAc in hexanes; R_f (33% EtOAc in hexanes) = 0.25) to routinely give an unequal mixture of diastereomers (3:1 mixture shown; 0.58 g, 2.7 mmol, 56%). ^{1}H NMR (500 MHz, $CDCl_3$, major diastereomer) δ 3.60 (m, 1H), 3.51 (m, 1H), 1.88 (dd, J=10.1, 4.0 Hz, 2H), 1.24 (br m), 1.51 (m), 0.97 (t, J= 7.4 Hz, 3H), 0.85 (t, J=6.9 Hz, 3H). ^{13}C NMR (125 MHz, $CDCl_3$) δ 76.4, 74.7, 32.1, 31.3, 29.9, 29.80, 29.79, 29.5, 26.2, 24.3, 22.9, 14.4, 10.7. IR ($CHCl_3$): 3415, 2929, 2856, 1456 cm^{-1}. HRMS (EI) calcd for $C_{13}H_{28}O_2$, 216.2089; found 216.2094 $[M]^+$.

4.6.2.2. 4-Hydroxytridecan-3-one (B3): To a solution of 2-ethyl-1,3-dithiane (2.0 g, 14 mmol) in THF (80 mL) at −15 °C was added *n*-butyllithium (2.5 M in hexanes, 6.0 mL, 15 mmol) dropwise. The mixture was stirred at −15 °C for 5 h. The mixture was cooled to −78 °C and a solution of decanal (1.66 g, 2.0 mL, 11 mmol) in THF (10 mL) was added dropwise. The reaction mixture was allowed to slowly reach 23 °C stirring overnight and was then poured onto 400 mL ice water, extracted with 3 × 150 mL DCM, washed with cold 2 N KOH (100 mL) and brine (100 mL). The organic layer was dried over $MgSO_4$, filtered, concentrated, and was used without further purification for the subsequent transformation. To a solution of *N*-chlorosuccinimide (1.76 g, 13.2 mmol) and silver(I) nitrate (2.53 g, 14.9 mmol) in 80% aqueous MeCN (100 mL) at 0 °C was added the above prepared 1-(2-ethyl-1,3-dithian-2-yl)decan-1-ol (0.940 g, 3.09 mmol) in MeCN (6 mL) in one portion. The reaction was stirred at 23 °C and monitored by TLC (20% EtOAc in hexanes). Upon completion, the reaction was quenched sequentially with 10 mL each saturated Na_2SO_3 (aq), saturated $NaHCO_3$ (aq), and saturated NaCl (aq). The reaction mixture was then poured onto 250 mL 1:1 hexanes/DCM and filtered through silica gel. The organic layer was recovered and dried over $MgSO_4$, filtered, concentrated, and purified by silica gel chromatography (20% EtOAc in hexanes; R_f = 0.44) to give α-hydroxyketone **B3** (0.093 g, 0.43 mmol, 14%). ^{1}H NMR (500 MHz, $CDCl_3$) δ 4.16 (m, 1H), 3.46 (d, J=4.9 Hz, 1H), 2.47 (m, 2H), 1.79 (m, 1H), 1.50 (m, 1H), 1.43 (m, 1H), 1.23 (m, 13H), 1.10 (t, J= 7.3 Hz, 3H), 0.85 (t, J = 6.9 Hz, 3H). ^{13}C NMR (125 MHz, $CDCl_3$) δ 213.1, 76.4, 34.1, 32.1, 31.3, 29.72, 29.67, 29.5, 25.0, 22.9, 14.3, 7.9. IR ($CHCl_3$): 3457, 2928, 2857, 1710 cm^{-1}. HRMS (EI) (m/z) M^+ calcd for $C_{13}H_{26}O_2$, 214.19328; found, 214.19377.

4.6.2.3. 4-Tridecanol (B4): A solution of distilled butyraldehyde (3.2 g, 4.0 mL, 44 mmol) in Et_2O (135 mL) was added dropwise to freshly prepared nonylmagnesium bromide (100 mL, 63 mmol, 0.63 M in Et_2O) dropwise over 30 min. The reaction was stirred at 23 °C overnight, quenched with saturated ammonium chloride (50 mL) at 0 °C, and filtered. The aqueous precipitate was extracted with DCM (3 × 50 mL). The organic layers were combined and washed with 100 mL each saturated ammonium chloride and brine. The organic layer was then dried over $MgSO_4$, filtered, concentrated, and purified by silica gel chromatography (5% EtOAc in hexanes; R_f (20% EtOAc in hexanes) = 0.52) to give alcohol **B4** (6.80 g, 33.9 mmol, 76%). The spectral data for **B4** is consistent with previously reported data for this compound.[16] ^{1}H NMR (500 MHz, CDCl3) δ 3.53 (s, 1H), 1.73 (br s, 1H), 1.35 (m, 6H), 1.22 (m, 14H), 0.87 (t, J= 7.0 Hz, 3H), 0.83 (t, J= 7.0 Hz, 3H). ^{13}C NMR (125 MHz, $CDCl_3$) δ 71.8, 39.9, 37.7, 32.1, 29.94, 29.85, 29.78, 29.5, 22.9, 19.0, 14.3, 14.2.

4.6.2.4. 4-Tridecanone (B5): A solution of 4-tridecanol (1.84 g, 9.18 mmol) in DCM (3 mL) was added to a solution of pyridinium chlorochromate (3.0 g, 14 mmol) in DCM (15 mL) at 0 °C dropwise over 5 min. The reaction was warmed to 23 °C and monitored by TLC (10% EtOAc in hexanes). Upon completion, 25 mL Et_2O were added and the supernatant was recovered. The residual black gum was rinsed with Et_2O (3 × 25 mL). The organic layers were then combined and filtered through a plug of silica gel, which was thoroughly

rinsed with ether. The ether layer was then dried over $MgSO_4$, filtered, concentrated, and purified by silica gel chromatography (10% EtOAc in hexanes; R_f = 0.45) to give 4-tridecanone (1.08 g, 5.46 mmol, 59%). The spectral data for **B5** is consistent with previously reported data for this compound.[17] ^{1}H NMR (500 MHz, $CDCl_3$) δ 2.35 (td, J = 7.4, 3.6 Hz, 4H), 1.57 (m, 4H), 1.26 (m, 12H), 0.88 (t, J = 7.4 Hz, 3H), 0.85 (t, J = 7.0, 3H). ^{13}C NMR (125 MHz, $CDCl_3$) δ 211.9, 44.9, 43.1, 32.1, 29.66, 29.65, 29.5, 24.1, 22.9, 17.5, 14.3, 14.0.

4.6.2.5. 3-Tridecanol (B6): Synthesis and purification followed that described for compound **B4,** utilizing propionaldehyde and decylmagnesium bromide (0.63 M in Et_2O) to give 3-tridecanol(3.77 g, 18.8 mmol, 34%). The spectral data for **B5** is consistent with previously reported data for this compound.[18] ^{1}H NMR (500 MHz, $CDCl_3$) δ 3.50 (m, 1H), 1.50 (m, 2H), 1.39 (m, 4H), 1.26 (m, 14H), 0.92 (t, J = 7.5 Hz, 3H), 0.86 (t, J = 6.9 Hz, 3H). ^{13}C NMR (125 MHz, $CDCl_3$) δ 73.6, 37.2, 32.1, 30.4, 29.94, 29.86, 29.84, 29.6, 25.9, 22.9, 14.4, 10.1. HRMS (EI) calcd for $C_{13}H_{28}O$, 200.2140; found, 200.2159 $[M]^+$.

4.6.2.6. 3-Tridecanone (B7): Synthesis and purification followed that described for compound **B5** using 3-tridecanol (**B6**) to give3-tridecanone (0.784 g, 3.95 mmol, 80%). The spectral data for **B7** is consistent with previously reported data for this compound.[19] ^{1}H NMR (500 MHz, $CDCl_3$) δ 2.39 (m, 4H), 1.52 (m, 2H), 1.23 (m, 14H), 1.03 (t, J = 7.3 Hz, 3H), 0.86 (t, J = 7.0 Hz, 3H). ^{13}C NMR(125 MHz, $CDCl_3$) δ 212.3, 42.7, 36.1, 32.1, 29.8, 29.7, 29.6, 29.53, 29.51, 24.2, 22.9, 14.3, 8.1.

4.6.3. Library C synthesis—For the synthesis of compounds **C5** and **C7**, see Ref. 13.

4.6.3.1. *2-(tert* -Butyldiphenylsilyloxy)dodecan-3-one (TBDPS-C1): Prepared from 2-(*tert*-butyldiphenylsilyloxy)-*N*-methoxy-*N*-methyl-propanamide[20] and nonyl-MgBr following the general procedure for Library A synthesis. Purified by silica gel chromatography (5% EtOAc in hexanes, R_f = 0.25) to give TBDPS-C1 (0.540 g, 1.23 mmol, 92%). ^{1}H NMR (500 MHz, CDCl3) δ 7.71 (m, 4H), 7.41(m, 6H), 4.20 (q, J =7.0 Hz, 1H), 2.53 (m, 2H), 1.48 (m, 2H), 1.28(m, 12H), 1.20 (d, J = 6.8 Hz, 3H), 1.11 (s, 9H), 0.90 (m, 3H).

4.6.3.2. 2-Hydroxydodecan-3-one (C1): To a solution of 2-(*tert*butyldiphenylsilyloxy) dodecan-3-one (0.49 g, 1.1 mmol) in THF(11 ml) at 0 °C, TBAF(5.6 ml, 5.6 mmol) was added slowly over 5 min. The reaction mixture was quenched after 30 min with NaH-CO_3 and diluted with ether (50 ml). The solution was then washed with water, dried with $MgSO_4$ and concentrated in vacuo. The residue was purified by preparative TLC (25% EtOAc in hexanes, R_f = 0.30). The product was extracted from the silica gel with diethyl ether and concentrated to give **C1** (0.040 g, 0.199 mmol, 18%). ^{1}H NMR (500 MHz, $CDCl_3$) δ 4.25 (m, 1H), 3.59 (s, 1H), 2.45 (m, 2H), 1.62 (m, 2H), 1.40 (m, 3H), 1.34 (m, 12H), 0.87 (m, 3H); ^{13}C NMR (125 MHz, $CDCl_3$) δ 212.7, 72.6, 37.6, 31.9, 29.4, 29.4, 29.3, 29.2, 23.6, 22.7, 19.9, 14.2. HRMS (EI) calcd for $C_{12}H_{24}O_2$, 200.1776; observed 200.1776 $[M]^+$.

4.6.3.3. Compounds C2–C4, C6–C7 and C9–C29; general procedure: The synthesis of compounds **C2–C4**, **C6–C7** and **C9–C29** followed that reported for Ph-CAI1.[13] To a solution of 2-nonyl-1,3-dithiane (1.0 equiv) in THF (0.5 M) at 0 °C was added *n*-BuLi (2.5 M soln. in hexanes, 1.0 equiv) and the resulting mixture was stirred for 4 h at 0 °C. This solution was added via syringe to a −78 °C solution of the aldehyde (1.0 equiv 1.0 M in THF), was allowed to warm to rt over 12 h and was quenched with 1.5 equiv H_2O. The resulting mixture was concentrated in vacuo to provide a slurry that was loaded onto a short plug of SiO_2 and eluted sequentially with a rapid gradient from hexanes to 50% EtOAc/Hex. The product containing fractions were combined and concentrated. The resulting

intermediate dithiane (>70% pure by ^{1}H NMR) was dissolved in ACN (0.5 M) and was cooled to 0 °C before treatment with a preformed solution of NCS (4.5 equiv) and $AgNO_3$ (5.0 equiv) in ACN/H_2O (80% ACN (aq), 0.18 M). The resulting cloudy solution was stirred at 0 °C for 15 min, quenched by the addition of saturated Na_2SO_3, diluted with Et_2O, extracted with Et_2O and dried over Na_2SO_4. Final purification was performed as described below utilizing flash column chromatography.

4.6.3.3.1. 4-Hydroxytetradecan-5-one (C2): Prepared according to the standard procedure utilizing 2-nonyl-1,3-dithiane and *n*-butanal. Purification was achieved using flash silica gel chromatography, gradient of hexanes to 5% EtOAc/Hex to give **C2** (0.030 g, 0.13 mmol, 42%). ^{1}H NMR (500 MHz, $CDCl_3$) δ 4.19 (d, *J*= 5 Hz, 1H), 3.50 (d, *J* = 4.9 Hz, 1H), 2.45 (m, 2H), 1.81 (m, 1H), 1.65 (m, 3H), 1.51 (m, 2H), 1.30 (m, 12H), 0.97 (m, 3H), 0.87 (m, 3H). ^{13}CNMR (125 MHz, $CDCl_3$) δ 212.8, 76.4, 38.1, 36.1, 32.1, 29.59, 29.55, 29.45, 29.43, 23.9, 22.9, 18.4, 14.3. LRMS (EI) calcd for $C_{14}H_{28}O_2$, 228; observed, 228 $[M]^+$, 199 $[M–C_2H_5]^+$, 186$[M–C_3H_6]^+$.

4.6.3.3.2. 3-Hydroxy-2-methyltridecan-4-one (C3): Prepared according to the standard procedure utilizing 2-nonyl-1,3-dithianeand isobutyraldehyde. Purification was achieved using flash silica gel chromatography, gradient of hexanes to 5% EtOAc/Hex to give **C3** (0.050 g, 0.22 mmol, 70%). ^{1}H NMR (300 MHz, $CDCl_3$) δ 4.08(d, *J* = 5 Hz, 1H), 3.42 (*J* = 4.8 Hz, 1H), 2.45 (t, *J* = 7.3 Hz, 2H), 2.15 (m, 1H), 1.62 (m, 2H), 1.26 (m, 12H), 1.12 (d, *J* = 6.6 Hz, 3H), 0.87 (br s, 3H), 0.71 (d, *J* = 6.7 Hz, 3H). ^{13}C NMR (125 MHz, $CDCl_3$) δ 207.4, 80.8, 38.3, 30.2, 29.6, 29.6, 29.5, 24.9, 23.8, 22.9, 20.0, 13.7, 13.1. LRMS (EI) calcd for $C_{14}H_{28}O_2$, 228; observed, 228 $[M]^+$, 213$[M–CH_3]^+$, 199 $[M–C_2H_5]^+$.

4.6.3.3.3. 3-Hydroxy-2,2-dimethyltridecan-4-one (C4): Prepared according to the standard procedure utilizing 2-nonyl-1,3-dithianeand pivalaldehyde. Purification was achieved using flash silica gel chromatography, gradient of hexanes to 5% EtOAc/Hex to give C4 (0.040 g, 0.15 mmol, 14%). ^{1}H NMR (500 MHz, $CDCl_3$) 3.80 (d, *J*= 5 Hz, 1H), 3.18 (d, *J* = 5 Hz, 1H), 2.43 (m, 2H), 1.65 (m, 2H), 1.19 (m, 12H), 0.91 (s, 9H), 0.81 (t, *J* = 5 Hz, 3H). ^{13}C NMR (125 MHz, $CDCl_3$) δ 213.6, 83.9, 42.2, 35.6, 31.9, 29.4, 29.3, 26.3, 24.0, 22.7, 14.1. LRMS (EI) calcd for $C_{15}H_{30}O_2$, 242; observed, 242$[M]^+$, 186 [M-*t*Bu]$^+$, 155 [M-C5H_{11}O]$^+$.

4.6.3.3.4. 1-Hydroxy-1-o-tolylundecan-2-one (C6): Prepared according to the standard procedure utilizing 2-nonyl-1,3-dithiane and **4**-methylbenzaldehyde. Purification was achieved using flash silica gel chromatography, gradient of hexanes to 5% EtOAc/Hex to give **C6** (0.60 g, 2.2 mmol, 57%). ^{1}H NMR (500 MHz, $CDCl_3$) δ 7.21 (m, 3H), 7.14 (m, 1H), 5.26 (d, *J* = 3.8 Hz, 1H), 4.30 (d, *J*= 3.8 Hz, 1H), 2.41 (s, 3H), 2.28 (m, 2H), 1.52 (m, 2H), 1.20 (m, 12H), 0.87 (t, *J* = 7.1 Hz, 3H). ^{13}C NMR (125 MHz, $CDCl_3$) δ 210.5, 136.7, 136.3, 131.5, 128.8, 128.7, 126.8, 77.8, 38.2, 32.0, 29.5, 29.4, 29.2, 23.9, 22.9, 19.6, 14.3. LRMS (EI) calcd for $C_{18}H_{28}O_2$, 276; observed, 276 $[M]^+$.

4.6.3.3.5. 1-Hydroxy-1-p-tolylundecan-2-one (C8): Prepared according to the standard procedure utilizing 2-nonyl-1,3-dithiane and 4-methylbenzaldehyde. Purification was achieved using flash silica gel chromatography, gradient of hexanes to 20% EtOAc/Hex to give **C8**. ^{1}H NMR (400 MHz, $CDCl_3$) δ 7.19 (m, 4H), 5.04 (s, 1H), 4.35 (br, 1H), 2.35 (s, 3H), 2.33 (m, 2H), 1.49 (m, 2H), 1.10–1.30 (m, 12H), 0.87 (t, *J*= 7 Hz, 3H). ^{13}C NMR (100 MHz, $CDCl_3$) δ 210.1, 138.7, 135.4, 129.9, 127.6, 79.7, 38.0, 32.1, 29.6, 29.4, 29.2, 23.9, 22.9, 21.4, 14.3. HRMS (EI) calcd for $C_{18}H_{28}O_2$, 276.20893; observed, 276.2089 $[M]^+$.

4.6.3.3.6. 1-Hydroxy-1-(3,4-dimethylphenyl)undecan-2-one (C9): Prepared according to the standard procedure utilizing 2-nonyl-1,3-dithiane and 3,4-dimethylbenzaldehyde.

Purification was achieved using flash silica gel chromatography, gradient of hexanes to 20% EtOAc/Hex to give **C9**. ^{1}H NMR (500 MHz, $CDCl_3$) δ 7.10 (d, J = 8.8 Hz, 1H), 7.02–7.00 (m, 2H), 4.99 (d, J = 4.4 Hz, 1H), 4.31 (d, J = 4.5 Hz, 1H), 2.40–2.26 (m, 2H), 2.23 (s, 6H), 1.53–1.40 (m, 2H), 1.31–1.02 (m, 12H), 0.84 (t, J = 7.1 Hz, 3H). ^{13}C NMR (125 MHz, $CDCl_3$) δ 210.3, 137.5, 137.3, 135.7, 130.3, 128.6, 125.2, 79.6, 37.9, 32.0, 29.1, 29.1, 29.0, 23.9, 22.8, 19.9, 19.7, 14.3. HRMS (ESI-TOF) calcd for $C_{19}H_{30}O_2Na$, 313.2143; observed, 313.2141 $[M+Na]^+$.

4.6.3.3.7. 1-(4-Ethylphenyl)-1-hydroxyundecan-2-one (C10): Prepared according to the standard procedure utilizing 2-nonyl-1,3-dithiane and 4-ethylbenzaldehyde. Purification was achieved using flash silica gel chromatography, gradient of hexanes to 20%EtOAc/Hex to give **C10** ^{1}H NMR (500 MHz, $CDCl_3$) δ 7.20–7.17 (m, 4H), 5.03 (s, 1H), 4.33 (s, 1H), 2.63 (q, J = 7.6 Hz, 2H), 2.39–2.19(m, 2H), 1.55–1.36 (m, 2H), 1.32–1.06 (m, 15H), 0.84 (t, J = 7.1 Hz, 3H). ^{13}C NMR (125 MHz, $CDCl_3$) δ 210.2, 145.0, 135.5, 128.6, 127.6, 79.6, 37.9, 32.0, 28.8, 28.7, 28.7, 28.6, 23.9, 22.9, 15.7, 14.3. HRMS (ESI-TOF) calcd for $C_{19}H_{30}O_2Na$, 313.2143; observed, 313.2142 $[M+Na]^+$.

4.6.3.3.8. 1-Hydroxy-1-(4-propylphenyl)-undecan-2-one (C11): Prepared according to the standard procedure utilizing 2-nonyl-1,3-dithiane and 4-propylbenzaldehyde. Purification was achieved using flash silica gel chromatography, gradient of hexanes to 10% EtOAc/Hex to give **C11**. ^{1}H NMR (400 MHz, $CDCl_3$) δ 7.20 (d, J = 8 Hz, 2H), 7.18 (d, J = 8 Hz, 2H), 5.05 (s, 1H), 2.58 (t, J = 7 Hz, 2H), 2.33 (m, 2H), 1.64 (m, 2H), 1.48 (m, 2H), 1.10–1.30 (m, 12H), 0.93 (t, J = 7 Hz, 3H), 0.87 (t, J = 7 Hz, 3H). ^{13}C NMR (100 MHz, $CDCl_3$) δ 210.2, 143.5, 135.6, 129.3, 127.6, 79.7, 38.1, 37.9, 32.1, 29.5, 29.4, 29.2, 24.7, 24.0, 22.9, 14.3, 14.0. HRMS (EI) calcd for $C_{20}H_{32}O_2$, 304.24023; observed 304.2402 $[M]^+$.

4.6.3.3.9. 1-Hydroxy-1-(2-hydroxyphenyl)undecan-2-one (C12): Prepared according to the standard procedure utilizing the 2-non-yl-1,3-dithiane and TBS protected 2-hydroxybenzaldehyde. Final deprotection was achieved under standard TBAF conditions (3.0 equiv TBAF, 1 M in THF, rt). Purification was achieved using flash silica gel chromatography, gradient of 20% EtOAc/Hex to 40% EtOAc/Hex to provide **C12** (0.025 g, 0.090 mmol, 33%). ^{1}H NMR (400 MHz, $CDCl_3$) δ 7.25 (m, 2H), 6.96 (m, 1H), 6.88 (m, 1H), 5.18 (s, 1H), 2.83 (s, 1H), 2.37 (m, 2H), 1.51 (m, 2H), 1.11 (m, 12H), 0.88 (t, J = 7.0 Hz, 3H). ^{13}C NMR (126 MHz, $CDCl_3$) δ 204.9, 149.9, 125.0, 124.3, 116.7, 115.5, 112.2, 73.8, 32.2, 26.6, 24.0, 23.9, 23.6, 18.3, 17.4, 8.9. HRMS (EI) calcd for $C_{17}H_{26}O_3$, 278.1882; observed 278.1881 $[M]^+$.

4.6.3.3.10. 1-Hydroxy-1-(3-hydroxyphenyl)undecan-2-one (C13): Prepared according to the standard procedure utilizing the 2-non-yl-1,3-dithiane and TBS protected 3-hydroxybenzaldehyde. Final deprotection was achieved under standard TBAF conditions (3.0 equiv TBAF, 1 M in THF, rt). Purification was achieved using flash silica gel chromatography, gradient of 20% EtOAc/Hex to 40% EtOAc/Hex to provide **C13** (0.02 g, 0.072 mmol, 27%). ^{1}H NMR (500 MHz, $CDCl_3$) δ 7.22 (t, J = 7.9 Hz, 1H), 6.86 (d, J = 7.6 Hz, 1H), 6.78 (dd, J = 8.1, 2.5 Hz, 1H), 6.73 (s, 1H), 5.93 (br s, 1H), 5.03 (s, 1H), 4.61 (br s, 1H), 2.36 (m, 2H), 1.50 (m, 2H), 1.22 (m, 12H), 0.87 (t, J = 7.0 Hz, 3H). ^{13}C NMR (125 MHz, $CDCl_3$) δ 209.9, 156.6, 139.4, 130.5, 112.0, 116.2, 114.3, 79.5, 38.0, 32.0, 29.5, 29.4, 29.1, 23.8, 22.9, 14.3. HRMS (EI) calcd for $C_{17}H_{26}O_3$, 278.1882; observed, 278.1879 $[M]^+$.

4.6.3.3.11. 1-Hydroxy-1-(4-hydroxyphenyl)undecan-2-one (C14): Prepared according to the standard procedure utilizing the 2-nonyl-1,3-dithiane and TBS protected 4-hydroxybenzaldehyde. Final deprotection was achieved under standard TBAF conditions (3.0 equiv TBAF, 1 M in THF, rt). Purification was achieved using flash silica gel

chromatography, gradient of 20% EtOAc/Hex to 40% EtOAc/Hex to provide **C14**. ^{1}H NMR (500 MHz, $CDCl_3$) δ 7.13 (d, δ = 8.1 Hz, 2H), 6.81 (d, J = 8.1 Hz, 2H), 5.13 (s, 1H), 5.00 (d, J = 3.9 Hz, 1H), 4.35 (d, J = 4.1 Hz, 1H), 2.36–2.21 (m, 2H), 1.57– 1.40 (m, 2H), 1.30–1.03 (m, 12H), 0.84 (t, J = 6.9 Hz, 3H); ^{13}C NMR (125 MHz, $CDCl_3$) δ 210.2, 156.2, 130.4, 129.2, 116.1, 79.2, 38.0, 32.0, 29.4, 29.3, 29.2, 23.9, 22.9, 14.3. HRMS (ESI-TOF) calcd for $C_{17}H_{26}O_3Na$, 301.1780; observed 301.1773 $[M+Na]^+$.

4.6.3.3.12. 1-Hydroxy-1-(3,4-dihydroxyphenyl)undecan-2-one(C15): Prepared according to the standard procedure utilizing the 2-nonyl-1,3-dithiane and bis-TBS protected 3,4-dihydroxy-benzaldehyde. Final deprotection was achieved under standard TBAF conditions (6.0 equiv TBAF, 1 M in THF, rt). Purification was achieved using flash silica gel chromatography, gradient of 20%EtOAc/Hex to 60% EtOAc/Hex to provide **C15**. ^{1}H NMR (500 MHz, $CDCl_3$) 6.88–6.75 (m, 1H), 6.75–6.63 (m, 2H), 5.83 (br s, 2H), 4.94 (s, 1H), 4.44 (br s, 1H), 2.37–2.23 (m, 2H), 1.78–1.56 (m, 2H), 1.56–1.40 (m, 2H), 1.33–1.06 (m, 10H), 0.84 (t, J = 6.7 Hz, 3H). ^{13}CNMR (125 MHz, $CDCl_3$) δ 210.2, 144.6, 144.2, 130.5, 120.8, 115.9, 114.4, 79.3, 37.9, 32.5, 29.6, 29.4, 29.4, 29.2, 23.9, 22.9, 14.3. HRMS (ESI-TOF) calcd for $C_{17}H_{26}O_4Na$, 317.1723; observed 317.1724 $[M+Na]^+$.

4.6.3.3.13. 1-Hydroxy-1-(2-methoxyphenyl)undecan-2-one (C16): Prepared according to the standard procedure utilizing 2-nonyl-1,3-dithiane and 2-methoxybenzaldehyde. Purification was achieved using flash silica gel chromatography, gradient of hexanes to 10% EtOAc/Hex to give **C16** (0.026 g, 0.089 mmol, 26%). ^{1}H NMR (500 MHz, $CDCl_3$) δ 7.35 (m, 1H), 7.24 (m, 1H), 6.97 (m, 1H), 6.91 (m, 1H), 5.38 (d, J = 4.7 Hz, 1H), 4.29 (d, J = 4.8 Hz, 1H), 3.85 (s, 3H), 2.33 (m, 2H), 1.51 (m, 2H), 1.15 (m, 12H), 0.87 (t, J = 6.8 Hz, 3H). ^{13}C NMR (125 MHz, $CDCl_3$) δ 209.0, 155.9, 128.8, 128.2, 125.5, 120.0, 110.0, 73.8, 54.4, 36.4, 30.8, 28.3, 28.2, 28.2, 28.0, 22.7, 21.6, 13.1. HRMS (EI) calcd for $C_{18}H_{28}O_3$, 292.2038; observed, 292.2038 $[M]^+$.

4.6.3.3.14. 1-Hydroxy-1-(3-methoxyphenyl)undecan-2-one (C17): Prepared according to the standard procedure utilizing 2-nonyl-1,3-dithiane and 3-methoxybenzaldehyde. Purification was achieved using flash silica gel chromatography, gradient of hexanes to 10% EtOAc/Hex to give **C17** (0.007 g, 0.024 mmol, 9%). ^{1}H NMR (500 MHz, $CDCl_3$) δ 7.23 (m, 1H), 6.80 (m, 3H), 4.98 (d, J = 4.4 Hz, 1H), 4.31 (d, J = 4.4 Hz, 1H), 3.74 (s, 3H), 2.27 (m, 2H), 1.42 (m, 2H), 1.11 (m, 12H), 0.80 (t, J = 6.9 Hz, 3H). ^{13}C NMR (125 MHz, $CDCl_3$) δ 208.5, 158.5, 139.6, 130.0, 119.9, 114.3, 112.6, 79.1, 55.3, 37.8, 31.9, 29.4, 29.2, 29.0, 23.7, 22.7, 14.2. HRMS (EI) calcd for $C_{18}H_{28}O_3$, 292.2038; observed, 292.2038 $[M]^+$.

4.6.3.3.15. 1-Hydroxy-1-(4-methoxyphenyl)-undecan-2-one (C18): Prepared according to the standard procedure utilizing 2-nonyl-1,3-dithiane and 4-methoxybenzaldehyde. Purification was achieved using flash silica gel chromatography, gradient of hexanes to 10% EtOAc/Hex to give **C18** (0.08 g, 2.7 mmol, 80%). ^{1}H NMR (500 MHz, $CDCl_3$) δ 7.22 (m, 2H), 6.86 (m, 2H), 5.05 (d, J = 9.5 Hz, 1H), 4.35 (d, J = 9.5 Hz, 1H), 3.81 (s, 3H), 2.31 (m, 2H), 1.50 (m, 2H), 1.20 (m, 12H), 0.87 (t, J = 7.1 Hz, 3H). ^{13}C NMR (125 MHz, $CDCl_3$) δ 210.2, 160.0, 130.3, 129.2, 114.7, 79.3, 55.5, 38.0, 32.0, 29.5, 29.4, 29.4, 29.1, 24.2, 22.8, 14.3. HRMS (EI) calcd for $C_{18}H_{28}O_3$ 292.2038; observed, 292.2037 $[M]^+$.

4.6.3.3.16. 1-(2-Fluorophenyl)-1-hydroxyundecan-2-one (C19): Prepared according to the standard procedure utilizing 2-nonyl-1,3-dithiane and 2-fluorobenzaldehyde. Purification was achieved using flash silica gel chromatography, gradient of hexanes to 20% EtOAc/Hex to give **C19**. ^{1}H NMR (500 MHz, $CDCl_3$) δ 7.35–7.04 (m, 4H), 5.39 (d, J = 4.4 Hz, 1H), 4.32 (d, J = 4.5 Hz, 1H), 2.47–2.23 (m, 2H), 1.55–1.42 (m, 2H), 1.34–1.06 (m, 12H), 0.84 (t, J = 7.1 Hz, 3H). ^{13}C NMR (125 MHz, $CDCl_3$) δ 209.1, 161.6, 159.6, 130.6, 129.0, 125.6,

124.9, 116.0, 73.3, 37.7, 32.0, 29.4, 29.3, 29.1, 23.8, 22.9, 14.3. HRMS (ESI-TOF) calcd for $C_{17}H_{25}FO_2Na$, 303.1736; observed 303.1732 $[M+Na]^+$.

4.6.3.3.17. 1-(3-Fluorophenyl)-1-hydroxyundecan-2-one (C20): Prepared according to the standard procedure utilizing the 2-nonyl-1,3-dithiane and 3-fluorobenzaldehyde. Purification was achieved using flash silica gel chromatography, gradient of Hexanes to 20% EtOAc/Hex to provide **C20**. ^{1}H NMR (500 MHz, $CDCl_3$) δ 7.37–7.28 (m, 1H), 7.10–7.05 (m, 1H), 7.05–6.96 (m, 2H), 5.04 (d, J = 4.0 Hz, 1H), 4.39 (d, J = 4.1 Hz, 1H), 2.42–2.23 (m, 2H), 1.57–1.39 (m, 2H), 1.33–1.04 (m, 12H), 0.84 (t, J = 7.1 Hz, 3H); ^{13}C NMR (125 MHz, $CDCl_3$) δ 209.2, 164.2, 162.2, 140.7, 130.7, 123.3, 115.8, 114.4, 79.2, 37.9, 32.0, 29.3, 29.2, 29.1, 23.8, 22.8, 14.3; HRMS (ESI-TOF) calcd for $C_{17}H_{26}FO_2$, 281.1917; observed 281.1914 $[M+H]^+$.

4.6.3.3.18. 1-(4-Fluorophenyl)-1-hydroxyundecan-2-one (C21): Prepared according to the standard procedure utilizing the 2-nonyl-1,3-dithiane and 4-fluorobenzaldehyde. Purification was achieved using flash silica gel chromatography, gradient of Hexanes to 20% EtOAc/Hex to provide **C21**. (0.035 g, 0.11 mmol, 42%).^{1}H NMR (500 MHz, $CDCl_3$) δ 7.30 (m, 2H), 7.80 (m, 2H), 5.06 (s, 1H), 4.36 (s, 1H), 2.31 (m, 2H), 1.50 (m, 2H), 1.14 (m, 12H), 0.87 (m, 3H). ^{13}C NMR (125 MHz, $CDCl_3$) δ 209.7, 162.1, 134.1 (d, J = 3.2 Hz), 129.4 (d, J = 8.3 Hz), 116.2 (d, J = 21.7 Hz), 79.1, 38.0, 32.0, 29.5, 29.4, 29.4, 29.1, 23.8, 22.9, 14.3. HRMS (EI) calcd for $C_{17}H_{25}FO_2$, 280.1839; observed 280.1838 $[M]^+$.

4.6.3.3.19. 1-(2,5-Difluorophenyl)-1-hydroxyundecan-2-one (C22): Prepared according to the standard procedure utilizing the 2-nonyl-1,3-dithiane and 2,5-difluorobenzaldehyde. Purification was achieved using flash silica gel chromatography, gradient of Hexanes to 20% EtOAc/Hex to provide **C22**. ^{1}H NMR (500 MHz, $CDCl_3$) δ 7.11–7.02 (m, 1H), 7.02–6.91 (m, 2H), 5.36 (s, 1H), 4.35 (br s, 1H), 2.49–2.25 (m, 2H), 1.58–1.46 (m, 2H), 1.35–1.08 (m, 12H), 0.84 (t, J = 7.0 Hz, 3H); ^{13}C NMR (125 MHz, $CDCl_3$) δ 208.4, 160.1, 158.2, 157.4, 155.5, 127.3, 127.2, 117.3, 117.1, 117.0, 116.9, 115.3, 115.1, 72.9, 37.7, 32.0, 29.4, 29.3, 29.1, 23.7, 22.8, 14.3. HRMS (ESI-TOF) calcd for $C_{17}H_{24}F_2O_2Na$, 321.1642; observed 321.1638$[M+Na]^+$.

4.6.3.3.20. 1-(2-Chlorophenyl)-1-hydroxyundecan-2-one (C23): Prepared according to the standard procedure utilizing the 2-non-yl-1,3-dithiane and 2-chlorobenzaldehyde. Purification was achieved using flash silica gel chromatography, gradient of Hexanes to 20% EtOAc/Hex to provide **C23**. ^{1}H NMR (500 MHz, $CDCl_3$) δ 7.40–7.37 (m, 1H), 7.30–7.15 (m, 3H), 5.54 (d, J = 4.1 Hz, 1H), 4.40 (d, J = 4.1 Hz, 1H), 2.47–2.20 (m, 2H), 1.59–1.38 (m, 2H), 1.32–1.04 (m, 12H), 0.82 (t, J = 6.9 Hz, 3H); ^{13}C NMR (125 MHz, $CDCl_3$) δ 209.2, 136.0, 133.7, 130.2, 130.0, 129.2, 127.7, 76.1, 38.0, 32.0, 29.4, 29.4, 29.2, 29.1, 23.8, 22.8, 14.3. HRMS (EI-TOF) calcd for $C_{17}H_{25}ClO_2Na$, 319.1435; observed 319.1435 $[M+Na]^+$.

4.6.3.3.21. 1-(3-Chlorophenyl)-1-hydroxyundecan-2-one (C24): Prepared according to the standard procedure utilizing the 2-nonyl-1,3-dithiane and 3-chlorobenzaldehyde. Purification was achieved using flash silica gel chromatography, gradient of Hexanes to 20% EtOAc/Hex to provide **C24**. ^{1}H NMR (500 MHz, $CDCl_3$) δ 7.35–7.26 (m, 3H), 7.22–7.15 (m, 1H), 5.02 (d, J = 4.1 Hz, 1H), 4.39 (d, J = 4.0 Hz, 1H), 2.42–2.21 (m, 2H), 1.57–1.36 (m, 2H), 1.34–1.04 (m, 12H), 0.84 (t, J = 7.0 Hz, 3H); ^{13}C NMR (125 MHz, $CDCl_3$) δ209.1, 140.3, 135.1, 130.4, 129.0, 127.7, 125.8, 79.2, 37.9, 32.0, 29.1, 29.1, 29.0, 23.8, 22.8, 14.3. HRMS (ESI-TOF) calcd for $C_{17}H_{25}ClO_2Na$, 319.1435; observed 319.1436 $[M+Na]^+$.

4.6.3.3.22. 1-(4-Chlorophenyl)-1-hydroxyundecan-2-one (C25): Prepared according to the standard procedure utilizing the 2-non-yl-1,3-dithiane and 4-chlorobenzaldehyde. Purification was achieved using flash silica gel chromatography, gradient of Hexanes to 20% EtOAc/Hex to provide **C25**. ^{1}H NMR (500 MHz, $CDCl_3$) δ 7.33 (d, J = 8.1 Hz, 2H), 7.24 (d, J = 7.8 Hz, 2H), 5.02 (d, J = 4.1 Hz, 1H), 4.37 (d, J = 4.1 Hz, 1H), 2.41–2.16 (m, 2H), 1.54–1.36 (m, 2H), 1.30–1.02 (m, 12H), 0.84 (t, J = 7.0 Hz, 3H); ^{13}C NMR (125 MHz, $CDCl_3$) δ 209.4, 136.8, 134.8, 129.4, 128.9, 79.2, 38.0, 32.0, 29.2, 29.2, 29.1, 29.1, 23.8, 22.9, 14.3. HRMS (ESI-TOF) calcd for $C_{17}H_{25}ClO_2Na$, 319.1435; observed 319.1435 $[M+Na]^+$.

4.6.3.3.23. 1-(2-Bromophenyl)-1-hydroxyundecan-2-one (C26): Prepared according to the standard procedure utilizing the 2-nonyl-1,3-dithiane and 2-bromobenzaldehyde. Purification was achieved using flash silica gel chromatography, gradient of Hexanes to 20% EtOAc/Hex to provide **C26**. ^{1}H NMR (500 MHz, $CDCl_3$) δ 7.58 (d, J = 8.0 Hz, 1H), 7.30 (m, 1H), 7.19 (m, 2H), 5.57 (d, J =4.0 Hz, 1H), 4.45 (d, J = 4.0 Hz, 1H), 2.50–2.23 (m, 2H), 1.58–1.41 (m, 2H), 1.33–1.09 (m, 12H), 0.84 (t, J = 7.0 Hz, 3H); ^{13}C NMR (125 MHz, $CDCl_3$) δ 209.3, 137.7, 133.6, 130.3, 129.3, 128.3, 124.1, 78.3, 38.2, 32.0, 29.4, 29.3, 29.1, 23.9, 22.9, 14.3. HRMS (EI-TOF) calcd for $C_{17}H_25BrO_2Na$, 363.0930 *m/z* (M+Na); observed 363.0929 $(M+Na)^+$.

4.6.3.3.24. 1-(3-Bromophenyl)-1-hydroxyundecan-2-one (C27): Prepared according to the standard procedure utilizing the 2-nonyl-1,3-dithiane and 3-bromobenzaldehyde. Purification was achieved using flash silica gel chromatography, gradient of Hexanes to 20% EtOAc/Hex to provide C27. ^{1}H NMR (500 MHz, $CDCl_3$) δ 7.50–7.37 (m, 1H), 7.32–7.16 (m, 3H), 5.02 (s, 1H), 4.37 (br s, 1H), 2.44–2.18 (m, 2H), 1.62–1.39 (m, 2H), 1.30–1.02 (m, 12H), 0.85 (t, J = 6.1 Hz, 3H); ^{13}C NMR (125 MHz, $CDCl_3$) δ 209.1, 140.5, 132.0, 130.7, 130.6, 126.3, 123.3, 79.2, 38.0, 32.0, 29.2, 29.1, 28.9, 23.8, 22.9, 14.4. HRMS (ESI-TOF) calcd for $C1_7H_{25}BrO_2Na$, 363.0930; observed 363.0927 $[M+Na]^+$.

4.6.3.3.25. 1-(4-Bromophenyl)-1-hydroxyundecan-2-one (C28): Prepared according to the standard procedure utilizing the 2-non-yl-1,3-dithiane and 4-bromobenzaldehyde. Purification was achieved using flash silica gel chromatography, gradient of hexanes to 20% EtOAc/Hex to provide **C28**.^{1}H NMR (500 MHz, $CDCl_3$) δ 7.51 (d, J = 8.5 Hz, 2H), 7.19 (d, J = 8.5 Hz, 2H), 5.03 (s, 1H), 4.39 (s, 1H), 2.31 (m, 2H), 1.49 (m, 2H), 1.10-1.30 (m, 12H), 0.87 (t, J= 7 Hz, 3H); ^{13}C NMR (125 MHz, $CDCl_3$) δ 209.3, 137.4, 132.3, 129.3, 123.0, 79.3, 38.0, 32.1, 29.5, 29.4, 29.2, 23.8, 22.9, 14.3. HRMS (ESI-TOF) calcd for $C_{17}H_{25}BrO_2Na$, 363.0930; observed 363.0930 $[M+Na]^+$.

4.6.3.3.26. 2-Hydroxy-1-phenyldodecan-3-one (C29): Prepared according to the standard procedure utilizing 2-nonyl-1,3-dithianeand 2-phenylacetaldehyde. Purification was achieved using flash silica gel chromatography, gradient of hexanes to 10% EtOAc/Hexto give **C29** (0.055 g, 0.199 mmol, 54%). ^{1}H NMR (500 MHz, $CDCl_3$) δ 7.32 (m, 3H), 7.24 (m, 2H), 4.41 (m, 1H), 3.43 (s, 1H), 3.14 (dd, J = 14.1, 4.6 Hz, 1H), 2.86 (dd, J = 14.1, 7.5 Hz, 1H), 2.46 (m, 2H), 1.58 (m, 2H), 1.23 (m, 12H), 0.89 (t, J = 7.0 Hz, 3H). ^{13}C NMR (125 MHz, $CDCl_3$)$^+$ 212.1, 137.0, 129.6, 128.9, 127.3, 77.5, 40.6, 39.0, 32.2, 29.8, 29.7, 29.6, 29.6, 23.9, 23.1, 14.5. HRMS (EI) calcd for $C_{18}H_{28}O_2$, 276.2089; observed, 276.2089 $[M]^+$.

4.6.3.4.1. tert-Butyl 2-(methoxy(methyl)amino)-2-oxo-1-phenyl-ethylcarbamate: A solution of 2-(*tert*-butoxycarbonylamino)-2-phenylacetic acid (1.0 g, 4.0 mmol) in DCM (10 mL) was cooled to 0 °C and 1,1′-carbonyl-diimidazole (0.542 g, 8.0 mmol) was added to the stirring mixture. The mixture was allowed to warm to room temperature overnight. The solution was then cooled to 0 °C and imidazole (1.29 g, 8.0 mmol), 4-DMAP (0.018 g,

0.012 mmol), and *N,O*-dimethylhydroxylamine hydrochloride (0.95 g, 8.0 mmol) were added. The solution was again allowed to warm to room temperature overnight. The reaction mixture was then diluted with DCM (15 mL), washed twice with 2N HCl (15 mL), once with brine (15 mL), dried over Na_2SO_4, concentrated, and purified by silica gel chromatography (25% EtOAc in hexanes, R_f = 0.30) to give *tert*-butyl 2-(methoxy(methyl)amino)-2-oxo-1-phenylethylcarbamate as colorless crystals (0.400 g, 1.36 mmol, 35%). ^{1}H NMR (500 MHz, $CDCl_3$) δ 7.25 (m, 5H), 5.72 (d, J = 7.7 Hz, 1H), 5.64 (d, J = 7.9 Hz, 1H), 3.39 (s, 3H), 3.11 (s, 3H), 1.33 (s, 9H). ^{13}C NMR (125 MHz, $CDCl_3$) δ 171.4, 155.2, 138.2,129.0, 128.3, 127.9, 79.9, 61.3, 55.2, 32.5, 28.5.

4.6.3.4.2. 1-(tert-Butoxycarbonylamino)-1-phenylundecan-2-one: In a dried flask, Mg^0 metal (0.7 g, 29 mmol) and ether (6.4 mL) were mixed with 1-bromononane (2.8 mL, 15 mmol) at room temperature. After the reaction mixture stopped bubbling it was allowed to stir for 30 min. The freshly prepared Grignard reagent was then transferred to another flask containing a solution of *tert*-butyl 2-(methoxy(methyl)amino)-2-oxo-1-phenylethylcarbamate (0.369 g, 1.25 mmol) in THF (15 mL). The reaction mixture was allowed to stir at room temperature overnight. Following dilution with diethyl ether (40 mL), the mixture was cooled to 0 °C and quenched with H_2O. The organic layer was seperated and was then washed with 10% $KHSO_4$ (2 × 40 mL), and brine (40 mL). The crude product was then dried with Na_2SO_4, filtered, concentrated, and purified by silica gel chromatography (25% EtOAc in hexanes, R_f = 0.65) to give 1-(*tert*-butoxycarbonylamino)-1-phenylundec-an-2-one as a white powder (0.420 g, 1.16 mmol, 80%). ^{1}H NMR (500 MHz, $CDCl_3$) δ 7.34 (m, 5H), 5.95 (d, J=6.1 Hz, 1H), 5.27 (d, J = 6.4 Hz, 1H), 2.35 (m, 2H), 1.51 (m, 2H), 1.40 (s, 9H), 1.15 (m, 12H), 0.91 (m, 3H).

4.6.3.4.3. 1-Aminohydrochloride-1-phenylundecan-2-one (C30): 1-(*tert*-Butoxycarbonylamino)-1-phenylundecan-2-one (0.240 g, 0.663 mmol) was dissolved in ether (4.5 mL) and HCl (1.4equiv, 12.1 M, 0.75 mL) was added to the solution. The mixture was stirred overnight and concentrated, and recrystallized from warm CHCl3 (0.012 g, 0.045 mmol, 7%). ^{1}H NMR (500 MHz, $CDCl_3$) δ 8.84 (s, 3H), 7.54 (m, 2H), 7.35 (m, 3H), 5.49 (s, 3H), 2.36 (m, 2H), 1.41 (m, 2H), 1.16 (m, 12H), 0.87 (t, J = 7.0 Hz, 3H). ^{13}C NMR (125 MHz, CDCl3) δ 203.8, 131.3, 129.8, 129.7, 129.6, 63.4, 39.4, 32.1, 29.6, 29.5, 29.5, 29.0, 23.3, 22.9, 14.3. HRMS (EI) calcd for $C_{18}H_{28}NO$, 262.21713; observed, 262.21713 $[M]^+$.

Supplementary Material

Refer to Web version on PubMed Central for supplementary material.

Acknowledgments

The authors acknowledge Yongfeng Li and Karen Jeng for their contributions to the synthesis of analog compounds, to Douglas Higgins for early work on the biological evaluation of agonist analogs, and to Lotus Separations, LLC (Christina Kraml) for essential contributions to compound purification and chiral resolution. This work was supported by the Howard Hughes Medical Institute, National Institutes of Health (NIH) grant 5R01AI054442, National Science Foundation (NSF) grant MCB-0343821 to BLB, NIH postdoctoral fellowship GM082061 to W.L.N. and the Dr. Horst Witzel Prize from Cephalon, Inc. (MEB).

References and notes

1. Waters CM, Bassler BL. Ann Rev Cell Dev Biol. 2005; 21:319. [PubMed: 16212498]
2. Cámara M, Williams P, Hardman A. Lancet Infect Dis. 2002; 2:667. [PubMed: 12409047]
3. Faruque SM, Islam MJ, Ahmad QS, Biswas K, Faruque ASG, Nair GB, Sack RB, Sack DA, Mekalanos JJ. J Infect Dis. 2006; 193:1029. [PubMed: 16518766]

4. Miller MB, Skorupski K, Lenz DH, Taylor RK, Bassler BL. Cell. 2002; 110:303. [PubMed: 12176318]
5. Chen X, Schauder S, Potier N, Van Dorsselaer A, Pelczer I, Bassler BL, Hughson FM. Nature. 2002; 415:545. [PubMed: 11823863]
6. Higgins DA, Pomianek ME, Kraml CM, Taylor RK, Semmelhack MF, Bassler BL. Nature. 2007; 450:883. [PubMed: 18004304]
7. Federle MJ, Bassler BL. J Clin Invest. 2003; 112:1291. [PubMed: 14597753]
8. Ng WL, Perez LJ, Wei Y, Kraml C, Semmelhack MF, Bassler BL. Mol Microbiol. 2011; 79:1407. [PubMed: 21219472]
9. Wei Y, Perez LJ, Ng WL, Semmelhack MF, Bassler BL. ACS Chem Biol. 2010; 6:356. [PubMed: 21197957]
10. Hammer BK, Bassler BL. Mol Microbiol. 2003; 50:101. [PubMed: 14507367]
11. Ng WL, Bassler BL. Annu Rev Genet. 2010; 43:197. [PubMed: 19686078]
12. Kelly RC, Bolitho ME, Higgins DA, Lu W, Ng WL, Jeffrey PD, Rabinowitz JD, Semmelhack MF, Hughson FM, Bassler BL. Nat Chem Biol. 2009; 5:891. [PubMed: 19838203]
13. Ng WL, Wei Y, Perez LJ, Cong J, Long T, Koch M, Semmelhack MF, Wingreen NS, Bassler BL. Proc Natl Acad Sci USA. 2010; 107:5575. [PubMed: 20212168]
14. Swem LR, Swem DL, Wingreen NS, Bassler BL. Cell. 2008; 134:461. [PubMed: 18692469]
15. Hunter CA, Sanders JKM. J Am Chem Soc. 1990; 112:5525.
16. Roush WR, Hoong LK, Palmer MA, Park JC. J Org Chem. 1990; 55:4109.
17. Ragagnin G, Betzemeier B, Quici S, Knochel P. Tetrahedron. 2002; 58:3985.
18. Hodgson DM, Fleming MJ, Stanway SJ. J Org Chem. 2007; 72:4763. [PubMed: 17530802]
19. Zhang D, Ready JM. Org Lett. 2005; 7:5681. [PubMed: 16321021]
20. Xie W, Zou B, Pei D, Ma D. Org Lett. 2005; 7:2775. [PubMed: 15957944]

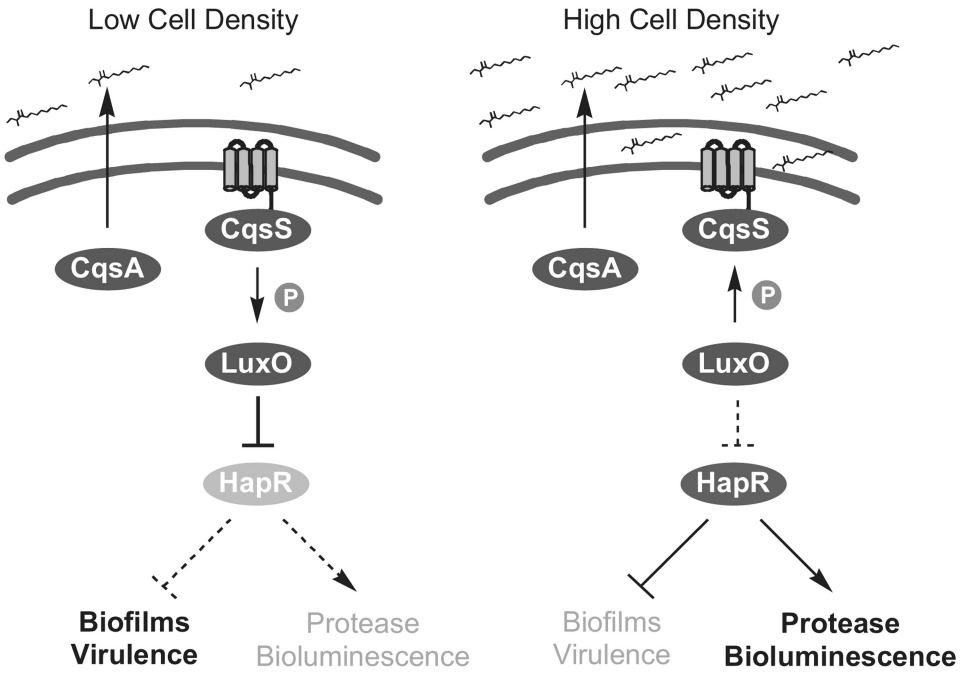

Figure 1.

Simplified diagram of the *Vibrio cholerae* CqsA/CqsS quorum sensing circuit. In the absence of CAI-1, for example at low cell density, biofilms are made, virulence factors are expressed, and protease production is repressed. In the presence of CAI-1, for example at high cell density, biofilm formation and virulence factor production are repressed, and a protease is produced. In our assay strain, bioluminescence is only induced in the presence of CAI-1. The P in the circle denotes phosphate flow. The full quorum-sensing relay mechanism is described in the text.

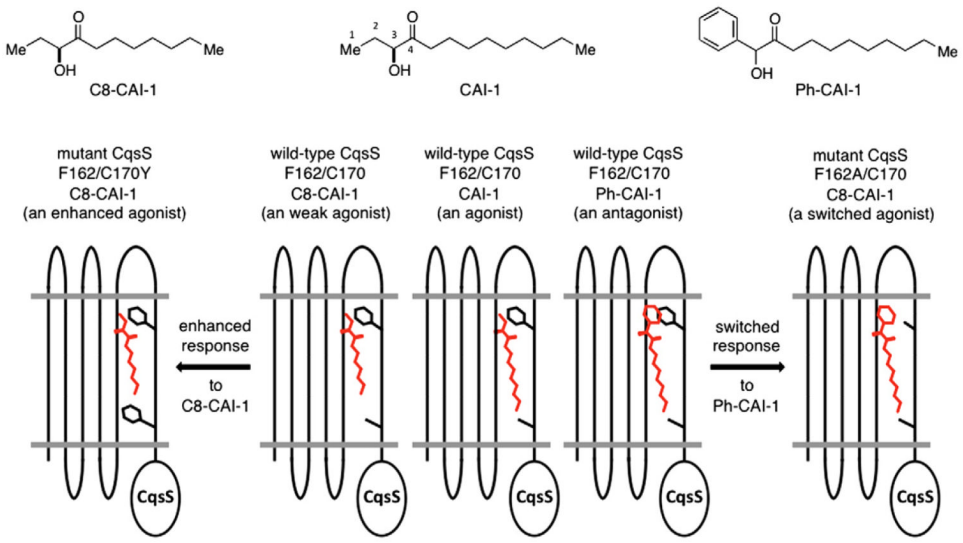

Figure 2.

Examples of molecules that modulate signaling in *V. cholerae* and a schematic representation of point mutants in CqsS that lead to altered signal specificity with the proposed orientation of the ligand. The ligand is shown in red and the side chains of residues 162 and 170 are shown in black.

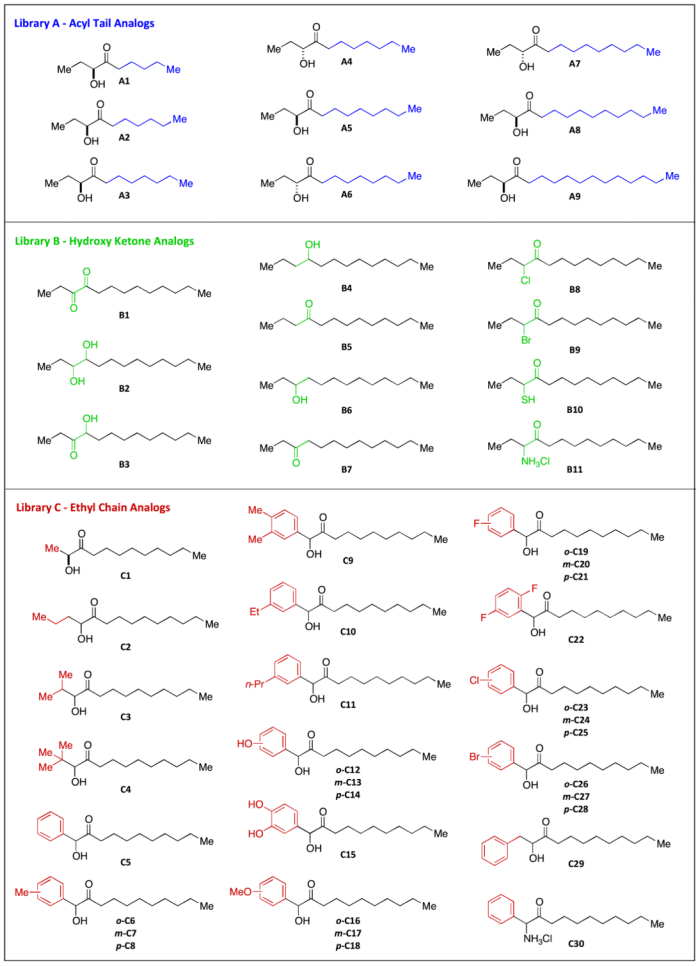

Figure 3.
Focused libraries of CAI-1 analogs.

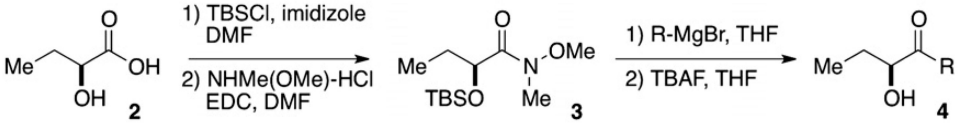

Scheme 1.
Synthesis of Library A.

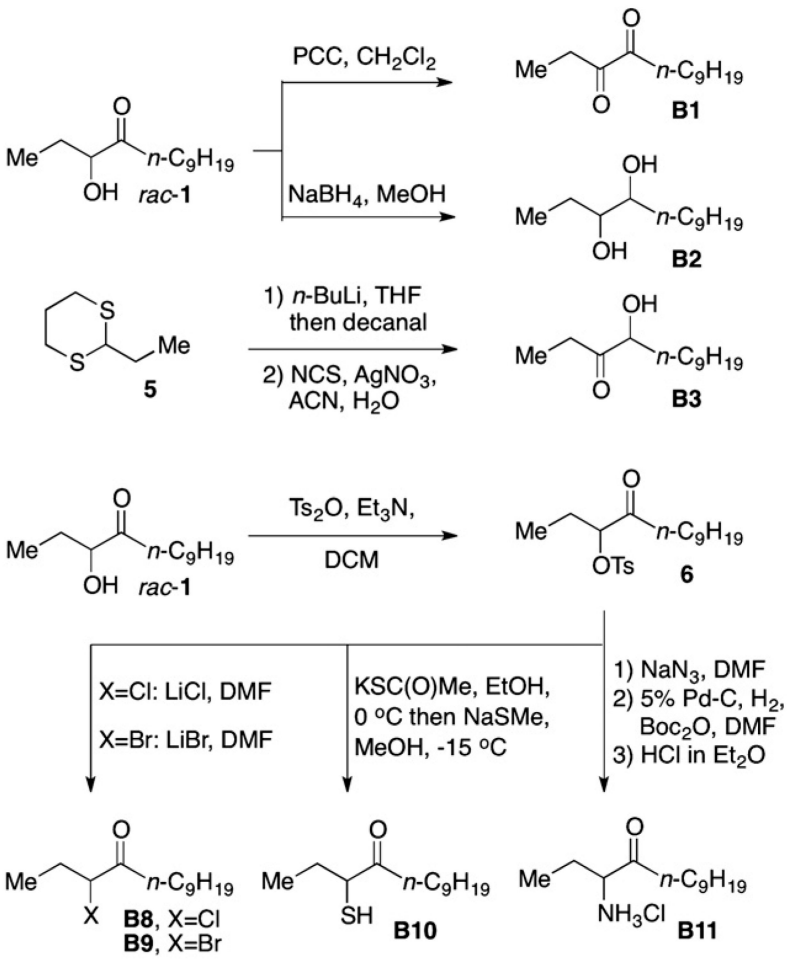

Scheme 2.
Synthesis of Library B.

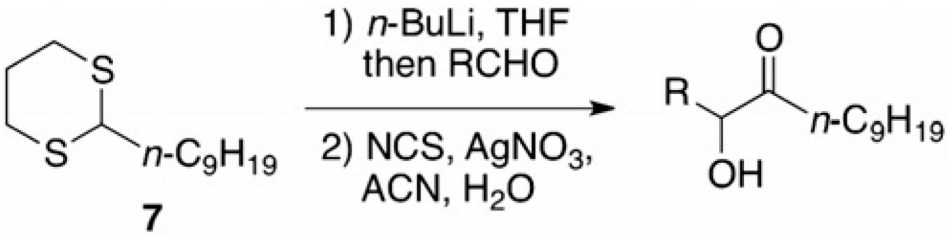

Scheme 3.
Synthesis of Library C.

Table 1

Agonist activities for Library A

Entry	Compound	EC_{50}[a] (μM)	% Response[c]	EC_{50} fold increase from CAI-1[d]
1	(*S*)-C6-CAI-1, **A1**	>50	27[e]	>200
2	(*S*)-C7-CAI-1, **A2**	>50	59[e]	>200
3a	(*S*)-C8-CAI-1, **A3**	9.45 ± 1.6[f]	83	39
3b	(*R*)-C8-CAI-1, **A4**	6.60 ± 2.1[f]	48	28
4a	(*S*)-C9-CAI-1, **A5**	1.10 ± 0.16[f]	100	4.6
4b	(*R*)-C9-CAI-1, **A6**	1.61 ± 0.07[f]	95	6.7
5a	(*S*)-CAI-1, **1**	0.25 ± 0.13[b]	100	–
5b	(*R*)-CAI-1, **A7**	0.64 ± 0.03[f]	100	2.7
6	(*S*)-C11-CAI-1, **A8**	2.09 ± 0.77[f]	98	8.4
7	(*S*)-C13-CAI-1, **A9**	>50	45[e]	>200

[a] Determined using a standard CqsS agonist bioassay, see Section 4. All EC_{50} values are the mean of triplicate analyses.

[b] The error is the standard error of means for EC_{50} values of CAI-1 determined on different days.

[c] Percent maximal bioluminescence, with respect to CAI-1 at 100%.

[d] The fold increase in EC_{50} (EC_{50} entry/EC_{50} CAI-1) calculated using the EC_{50} value of CAI-1 determined on the same day.

[e] % Response at the maximum concentration (50 μM).

[f] 95% Confidence interval.

Table 2

Agonist activities for Library B

Entry	Compound	EC_{50}[a] (μM)	% Response[c]	EC_{50} fold increase from CAI-1[d]
1	(*S*)-CAI-1, **1**	0.25 ± 0.13[b]	100	n.a.
2	Diketone-CAI-1, **B1**	3.2 ± 0.27[e]	92	14
3	Diol-CAI-1, **B2**	4.3 ± 0.40[e]	83	18
4	3-Keto-4-hydroxy-CAI-1, **B3**	21 ± 3.6[e]	38	84
5	4-Tridecanol, **B4**	>50	n.a.	>200
6	4-Tridecanone, **B5**	>50	n.a.	>200
7	3-Tridecanol, **B6**	>50	n.a.	>200
8	3-Tridecanone, **B7**	>50	n.a.	>200
9	Cl-CAI-1, **B8**	>50	24	>200
10	Br-CAI-1, **B9**	2.4 ± 1.8[e]	73	13
11	SH-CAI-1, **B10**	1.6 ± 0.77[e]	67	8.6
12	NH_2-CAI-1, **B11**	0.21 ± 0.01[e]	105	0.27

[a] Determined using a standard CqsS agonist bioassay, see Section 4. All EC_{50} values are the mean of triplicate analyses.

[b] The error described here is the standard error of means for EC_{50} values of CAI-1 determined on different days.

[c] Percent maximal bioluminescence, with respect to CAI-1 at 100%.

[d] The fold increase in EC_{50} (EC_{50} entry/EC_{50} CAI-1) calculated using the EC_{50} value of CAI-1 determined on the same day.

[e] 95% Confidence interval. n.a. = not applicable.

Table 3

Agonist activities for Library C

Entry	Compound	EC_{50}[a] (μM)	% Response[c]	EC_{50} fold increase from CAI-1[d]
1	Me-CAI-1, **C1**	0.34 ± 0.06[e]	96	2.6
2	(*S*)-CAI-1, **1**	0.25 ± 0.13[b]	100	n.a.
3	*n*-Pr-CAI-1, **C2**	0.78 ± 0.17[e]	84	6.0
4	*i*-Pr-CAI-1, **C3**	7.16 ± 11[e]	71	21
5	*t*-Bu-CAI-1, **C4**	>50	n.a.	>200

[a] Determined using a standard CqsS agonist bioassay, see Section 4. All EC_{50} values are the mean of triplicate analyses.

[b] The error described here is the standard error of means for EC_{50} values of CAI-1 determined on different days.

[c] Percent maximal bioluminescence, with respect to CAI-1 at 100%.

[d] The fold increase in EC_{50} (EC_{50} entry/EC_{50} CAI-1) calculated using the EC_{50} value of CAI-1 determined on the same day.

[e] 95% confidence interval. n.a. = not applicable.

Table 4

Antagonist activities for Library C

Entry	Compound	IC_{50}[a] (μM)	% Inhibition[c]	Ratio: IC_{50} (analog)/IC_{50} (Ph-CAI-1)[d]
1	Ph-CAI-1, **C5**	55 ± 15[b]	100	1.0
2	*o*-Me-Ph-CAI-1, **C6**	>500	n.a.	>9
3	*m*-Me-Ph-CAI-1, **C7**	46 ±8.2[e]	58	0.91
4	*p*-Me-Ph-CAI-1, **C8**	114± 65[e]	99	2.2
5	3,4-di-Me-Ph-CAI-1, **C9**	>500	n.a.	>9
6	*p*-Et-CAI-1, **C10**	>500	n.a.	>9
7	*p*-Pr-CAI-1, **C11**	>500	n.a.	>9
8	*o*-OH-Ph-CAI-1, **C12**	172 ± 52[e]	144	3.4
9	*m*-OH-Ph-CAI-1, **C13**	36 ±3.3[e]	123	0.71
10	*p*-OH-Ph-CAI-1, **C14**	78 ±9.2[e]	119	1.5
11	3,4-di-OH-Ph-CAI-1, **C15**	174± 21[e]	122	3.4
12	*o*-OMe-Ph-CAI-1, **C16**	>500	n.a.	>9
13	*m*-OMe-Ph-CAI-1, **C17**	>500	n.a.	>9
14	*p*-OMe-Ph-CAI-1, **C18**	>500	n.a.	>9
15	*o*-F-Ph-CAI-1, **C19**	74 ± 10[e]	105	1.5
16	*m*-F-Ph-CAI-1, **C20**	178 ± 54[e]	112	3.5
17	*p*-F-Ph-CAI-1, **C21**	137 ± 31[e]	125	2.7
18	2,5-di-F-Ph-CAI-1, **C22**	68 ±47[e]	48	1.3
19	*o*-Cl-Ph-CAI-1, **C23**	>500	n.a.	>9
20	*m*-Cl-Ph-CAI-1, **C24**	>500	n.a.	>9
21	*p*-Cl-Ph-CAI-1, **C25**	>500	n.a.	>9
22	*o*-Br-Ph-CAI-1, **C26**	>500	n.a.	>9
23	*m*-Br-Ph-CAI-1, **C27**	>500	n.a.	>9
24	*p*-Br-Ph-CAI-1, **C28**	185 ± 61[e]	71	2.6
25	Bn-CAI-1, **C29**	136± 21[e]	124	1.9
26	Ph-Am-CAI-1, **C30**	>500	n.a.	>9

[a] Determined using a standard CqsS agonist bioassay, see Section 4. All IC_{50} values are the mean of triplicate analyses.

[b] The error described here is the standard error of means for IC_{50} values of Ph-CAI-1 determined on different days.

[c] Percent maximal bioluminescence inhibition, with respect to Ph-CAI-1 at 100%.

[d] The fold increase in IC_{50} (IC_{50} entry/IC_{50} Ph-CAI-1) calculated using the IC_{50} value of Ph-CAI-1 determined on the same day.

[e] 95% Confidence interval. n.a. = not applicable.